Sequential bond energies and barrier heights for the water loss and charge separation dissociation pathways of Cd2+(H2O)n, n = 3–11

Theresa E. Cooper and P. B. Armentrout

Citation: J. Chem. Phys. **134**, 114308 (2011); doi: 10.1063/1.3553813
View online: http://dx.doi.org/10.1063/1.3553813
View Table of Contents: http://jcp.aip.org/resource/1/JCPSA6/v134/i11
Published by the American Institute of Physics.

Sequential bond energies and barrier heights for the water loss and charge separation dissociation pathways of $Cd^{2+}(H_2O)_n$, $n = 3–11$

Theresa E. Cooper and P. B. Armentrout[a)]
Department of Chemistry, University of Utah, 315 S. 1400 E. Rm 2020, Salt Lake City, Utah 84112, USA

(Received 29 November 2010; accepted 21 January 2011; published online 17 March 2011)

The bond dissociation energies for losing one water from $Cd^{2+}(H_2O)_n$ complexes, $n = 3–11$, are measured using threshold collision-induced dissociation in a guided ion beam tandem mass spectrometer coupled with a thermal electrospray ionization source. Kinetic energy dependent cross sections are obtained for $n = 4–11$ complexes and analyzed to yield 0 K threshold measurements for loss of one, two, and three water ligands after accounting for multiple collisions, kinetic shifts, and energy distributions. The threshold measurements are converted from 0 to 298 K values to give the hydration enthalpies and free energies for sequentially losing one water from each complex. Theoretical geometry optimizations and single point energy calculations are performed on reactant and product complexes using several levels of theory and basis sets to obtain thermochemistry for comparison to experiment. The charge separation process, $Cd^{2+}(H_2O)_n \rightarrow CdOH^+(H_2O)_m + H^+(H_2O)_{n-m-1}$, is also observed for $n = 4$ and 5 and the competition between this process and water loss is analyzed. Rate-limiting transition states for the charge separation process at $n = 3–6$ are calculated and compared to experimental threshold measurements resulting in the conclusion that the critical size for this dissociation pathway of hydrated cadmium is $n_{crit} = 4$. © *2011 American Institute of Physics*. [doi:10.1063/1.3553813]

I. INTRODUCTION

Cadmium is an especially toxic and environmentally hazardous substance, whose anthropogenic emissions have been categorized to be 18 times higher than naturally occurring rates.[1,2] Because cadmium can deactivate important proteins and enzymes, bioaccumulate, and has a biological half-life of 10–30 years, the United States environmental protection agency has classified cadmium as a priority pollutant. With such a large anthropogenic discharge into the environment, cadmium is quickly breaching valuable aqueous resources around the world, particularly in industrialized countries. An accurate and complete understanding of the thermochemical properties and reaction pathways of $Cd^{2+}(H_2O)_n$ complexes is necessary for the efficient removal of this metal pollutant from these aqueous systems.

The hydration of metal cations, both singly and multiply charged, has been studied extensively in the gas phase over the past two decades.[3–16] Such studies had never included the thermochemistry for hydration of cadmium until a recent article[17] in which we experimentally examined $Cd^{2+}(H_2O)_n$, $n = 4–11$, and discussed previous experimental and theoretical work[18–25] on cadmium coordination behavior. This study focused on the dominant reaction pathway, primary water loss in reaction (1).

$$Cd^{2+}(H_2O)_n \rightarrow Cd^{2+}(H_2O)_{n-1} + H_2O. \quad (1)$$

This is followed by sequential loss of additional water molecules at higher energies. As will be seen below, particular sized complexes also undergo a charge separation process, reaction (2).

$$Cd^{2+}(H_2O)_n \rightarrow CdOH^+(H_2O)_m + H^+(H_2O)_{n-m-1}. \quad (2)$$

The latter reaction is observed as a primary dissociation channel only for complexes of $n = 4$ and 5. In the present paper, we examine the competition between reactions (1) and (2) in detail, thereby providing further thermodynamic information for both channels.

Similar to the hydration of $Zn^{2+}(H_2O)_n$,[7,26–32] the ground state (GS) structures and coordination number (CN) for hydrated Cd^{2+} are highly dependent on the level of theory used. Our preliminary report[17] on $Cd^{2+}(H_2O)_n$ explored the experimental dissociation pathways as predicted by MP2(full)/SD/6-311+G(2d,2p)//B3LYP/SD/6-311+G(d,p) [with the Stuttgart–Dresden (SD) effective core potential (ECP) and basis set for Cd][33] calculations of the low-energy structures and found an excellent agreement between experimental and theoretical bond energies for water loss. These results indicate CN = 6, whereas B3LYP/SD/6-311+G(2d,2p)//B3LYP/SD/6-311+G(d,p) low-energy structures of $Cd^{2+}(H_2O)_n$ have a smaller primary hydration shell (CN = 4 or 5, depending on complex size). As shown previously,[26] our experimental thermochemistry can rely on the specific isomer considered, specifically how many inner shell versus outer shell water ligands are present in the reactants and products. In order to obtain a complete understanding of the Zn^{2+} hydration energies, we reported multiple bond dissociation energies (BDEs) for $Zn^{2+}(H_2O)_n$, where $n = 6–10$, based on differing low-energy structures predicted at MP2(full) and B3LYP levels. Results from this previous study combined with a recent infrared photodissociation

a)Author to whom correspondence should be addressed. Electronic mail: armentrout@chem.utah.edu.

spectroscopy investigation[34] on $Zn^{2+}(H_2O)_n$, where $n = 6–12$, support the GS structures predicted at the MP2(full) level over those predicted at the B3LYP and B3P86 levels. Consequently, in the present work, the thermochemical properties of $Cd^{2+}(H_2O)_n$, $n = 3–11$, are based on the GS structures predicted at the MP2(full) level using two different basis sets.

Compared to our previous report,[17] we have recalculated the $Cd^{2+}(H_2O)_n$ structures at the B3LYP/SD/6-311+G(d,p) level to ensure that they are fully converged after the frequency calculation. We also perform additional optimization and single point energy calculations using a size-consistent basis set for all atoms (Def2TZVP and Def2TZVPP).[35] Ultimately, the analysis performed in the present study finds the threshold energies reported earlier for reaction (1) remain essentially the same, but now includes additional thermochemical results and discussions of the cross sections and competition between reactions (1) and (2). Additionally, the new theoretical results are compared with the corresponding primary thresholds for reaction (1).

II. EXPERIMENTAL AND THEORETICAL SECTION

A. Experimental procedures

The experimental methods used to form the $Cd^{2+}(H_2O)_n$ complexes and obtain the kinetic energy dependent cross sections for the collision-induced dissociation (CID) are described in detail elsewhere.[17] Briefly, the complexes are formed at room temperature in an electrospray ionization (ESI) source coupled with an ion funnel and radio frequency hexapole ion guide. An in-source fragmentation technique, utilizing electrodes in the hexapole region of our source,[36] was used to increase the amount of the $n = 4–6$ complexes produced by our ESI source. Increasing the voltage on the electrodes enhances the intensity of smaller metal hydrate complexes as described previously for $Ca^{2+}(H_2O)_n$ complexes;[36] however, for $Cd^{2+}(H_2O)_n$ complexes, increasing the electrode voltage past the intensity peak for the $n = 4$ complex generates only charge separation products with no hydrated complexes smaller than $n = 4$ being observed. After mass selection, complexes are collided at varying pressures of Xe (typically about 0.05, 0.10, and 0.20 mTorr) and intensities of the reactant and product ions are measured. Product and reactant ion intensities as a function of the ion kinetic energy in the lab frame are converted to absolute cross sections as a function of relative energy and are extrapolated to zero pressure to ensure single collision conditions, as outlined elsewhere.[37–39]

B. Threshold analysis

Competition between reactions (1) and (2) can be modeled statistically using equations described elsewhere.[40] These methods include three adjustable parameters: $\sigma_{0,j}$ which is an energy-independent scaling factor for channel j, N which is an adjustable parameter that describes the efficiency of collisional energy transfer,[41] and $E_{0,j}$ which is the threshold for CID of the ground electronic and rovibrational state of the reactant ion at 0 K for channel j. The model incorporates Rice–Ramsperger–Kassel–Marcus (RRKM) theory[42,43] to describe the kinetics of the competitive dissociations.[44–46] Rotational constants and vibrational frequencies needed in the analyses are taken from quantum chemical calculations discussed below. Because the charge separation process in reaction (2) produces two singly charged species, there must be an associated Coulomb barrier along the reactant coordinate for this dissociation channel, such that the appropriate transition state (TS) is tight. The rate limiting TSs of reaction (2) are labeled according to the products formed, i.e., TS$[m + (n - m - 1)]$. For the water loss channels of reaction (1), the TS is loose because the bond cleavage is heterolytic with all the charge remaining on the fragment containing the cadmium ion.[47] This TS is treated at the phase space limit in which the TS is product like and the transitional modes are treated as rotors.[46]

Thresholds for sequential dissociation of a second water molecule were modeled in conjunction with that of the single water loss channel, reaction (1). A statistical approach to modeling sequential dissociation has recently been developed and proven to provide accurate thresholds for singly charged systems[48] and $Zn^{2+}(H_2O)_n$.[26,49] Because of the complexity of the sequential dissociation model, its use is presently limited to a single primary product channel such that a "sequential competitive" model is not included in our analysis.

Analysis of the data involves using equations described elsewhere to reproduce the data over extended energy and magnitude ranges, using a least-squares criterion for optimizing the fitting parameters, $\sigma_{0,j}$, $E_{0,j}$, and N. The uncertainties in these parameters include variations associated with modeling several independent experimental cross sections, scaling the theoretical vibrational frequencies by ±10%, varying the optimum N value by ±0.1, scaling the experimental time of flight up and down by a factor of two, and the uncertainty in the absolute energy scale (0.05 eV Lab).

C. Quantum chemical calculations

Calculations were performed using the GAUSSIAN 03 package,[50] with full details described in our previous paper.[17] Briefly, geometry optimizations were performed at the B3LYP (Ref. 51, 52) level of theory with a 6-311+G(d,p) basis set on the waters and the Stuttgart–Dresden ECP and basis set on Cd^{2+}. For comparison to our previous calculations, geometry optimizations were also performed at the B3LYP/Def2TZVP level, where the Def2TZVP basis set includes triple zeta + polarization functions and the SD ECP. Both basis sets and ECPs were obtained from the EMSL basis set exchange[53] and have a small effective core of 28 electrons for Cd.[33] Vibrational frequencies and rotational constants were also calculated at both levels of theory. Since our previous report[17] on this system, additional calculations have been performed to ensure that each structure is fully converged after the frequency calculation. In addition, the tight TSs of the charge separation processes were obtained using TS optimization calculations at the B3LYP/Def2TZVP level and were found to have one imaginary frequency. Calculations of the TS for reaction (2) using the SD/6-311+G(d,p)

basis set failed, yielding more than one negative frequency or unreasonable structures. The benefit of the Def2TZVP (as well as Def2TZVPP) basis sets is that they are balanced basis sets for all atoms, which could be the reason the SD/6-311+G(d,p) basis set failed for these tight TS calculations. All other structures were found to be vibrationally stable using either basis set. Frequencies were scaled by 0.989 (Ref. 54) before being used in the RRKM analysis described above and in the calculation of the zero point energy (ZPE) and thermal corrections. The optimized parameters of the water loss pathways modeled were not dependent on whether the frequencies used in the modeling were calculated with the Def2TZVP or SD/6-311+G(d,p) basis set. Single point energies were calculated at the B3LYP, B3P86,[55] and MP2(full) (Ref. 56) levels of theory using the SD/6-311+G(2d,2p) and Def2TZVPP basis sets. Basis set superposition error corrections were calculated for reaction (1) in the full counterpoise (cp) limit.[57,58]

III. RESULTS AND DISCUSSION

A. CID cross sections

Experimental cross sections for collision-induced dissociation with Xe were acquired for $Cd^{2+}(H_2O)_n$, $n = 4$–11, Fig. 1. In all cases the loss of a single water molecule, reaction (1), is the dominant process, followed by loss of additional water molecules as the translational energy increases. The individual products for reactions (1) and (2) are shown in Figs. 1(a)–1(c), the cases where reaction (2) complicates the dissociation of $Cd^{2+}(H_2O)_5$, $Cd^{2+}(H_2O)_4$, and possibly $Cd^{2+}(H_2O)_3$. The total cross section of all charge separation products is shown in Figs. 1(d)–1(f), because in these three systems, these products do not compete with the two lowest energy water loss channels. Only the sequential water loss products from the dissociation of $Cd^{2+}(H_2O)_{10}$ and $Cd^{2+}(H_2O)_{11}$ are shown in Figs. 1(g) and 1(h), respectively. At these larger complex sizes, the charge separation products were not observed because the reactant ion intensity is small as is the extent of fragmentation to yield charge separation products.

B. $n = 4$

Cross sections for reaction (1) with $Cd^{2+}(H_2O)_4$ have been discussed previously,[17] but little attention was given to reaction (2) and its products. The $Cd^{2+}(H_2O)_4$ reactant dissociates via both reactions (1) and (2), Fig. 1(a). The lowest energy charge separation process observed corresponds to reaction (3),

$$Cd^{2+}(H_2O)_4 + Xe \rightarrow CdOH^+(H_2O)_2 + H^+(H_2O) + Xe, \quad (3)$$

which has a lower apparent threshold than that for formation of $Cd^{2+}(H_2O)_3$ in reaction (1). This observation along with the quantitative thresholds presented below show that reaction (3) is thermodynamically favored over reaction (1). Because of this, our thermal ESI source is limited to producing reactant ions of $n \geq 4$, as discussed in detail previously for the hydrated Zn^{2+} system.[26,49] Despite being energetically favored, the magnitude of the cross section for charge separation is smaller compared to that for water loss above about 1.3 eV, clearly indicating that charge separation is an entropically disfavored reaction. Although the loss of H_2O is energetically more costly than reaction (3), the relative threshold difference between the two dissociation pathways is small and reaction (1) is entropically favored thereby allowing the observation of $Cd^{2+}(H_2O)_3$ and $Cd^{2+}(H_2O)_2$ complexes at high collision energies in our CID experiments [Figs. 1(b)–1(f)].

The magnitudes of the cross sections for $CdOH^+(H_2O)_2$ and $H^+(H_2O)$ formed in reaction (3) should be identical, but that for the protonated water cluster is smaller than that of its hydrated cadmium hydroxide cation partner. Similar observations are made in all systems examined here, Figs. 1(a)–1(c), and previously[49] for zinc dication hydrates. This difference is a result of the lower collection efficiency of the lighter product ion. Because the products of the charge separation process pass over a large Coulomb barrier, there is considerable kinetic energy release in the product channel. In particular, the lighter product ion can have large kinetic energies that can exceed the center of mass velocity, meaning that a portion of these ions can travel backwards in the laboratory frame and are lost at the entrance to the octopole ion guide under the focusing conditions usually used. Focusing conditions in which such backward scattered products are reflected at the entrance and therefore collected at the detector can be used and demonstrate that the protonated water cross sections increase to match those of the hydrated metal hydroxide cation. Under such conditions, the cross sections of all heavy ion products (i.e., the singly charged hydrated metal hydroxide and the doubly charged hydrated metal) are unaffected. However, these focusing conditions greatly lower the overall reactant ion intensity, leading to an increase in the total experimental collection time and reduced signal-to-noise ratio. Therefore, the data shown are collected under standard focusing conditions with the understanding that the hydrated metal hydroxide cation cross section is the more accurate determination of the absolute cross section for the charge separation processes.

The $CdOH^+(H_2O)_2$ product cross section decreases above 1.8 eV, indicating that it must be dissociating, as also indicated by the observance of $CdOH^+(H_2O)$. The onset in the $CdOH^+(H_2O)$ product cross section exhibits a pressure effect, such that the low energy feature below 1.8 eV disappears upon extrapolation to zero pressure, Fig. 1(a). Above about 2.4 eV in Fig. 1(a), there is a 40% increase in the $H^+(H_2O)$ product cross section, observed more easily on a linear y-axis scale, that is mirrored in the sum of the cadmium hydroxide product cross sections. This increase is believed to correspond to reaction (4).

$$Cd^{2+}(H_2O)_3 + Xe \rightarrow CdOH^+(H_2O) + H^+(H_2O) + Xe. \quad (4)$$

This reaction is plausible because the charge separation process should be energetically favored over the loss of a water ligand for all complexes smaller than $n = 4$, a trend discussed previously for the related zinc system.[49] Therefore, the $CdOH^+(H_2O)$ product cross section can have contributions from both reaction (4) and water ligand loss from the

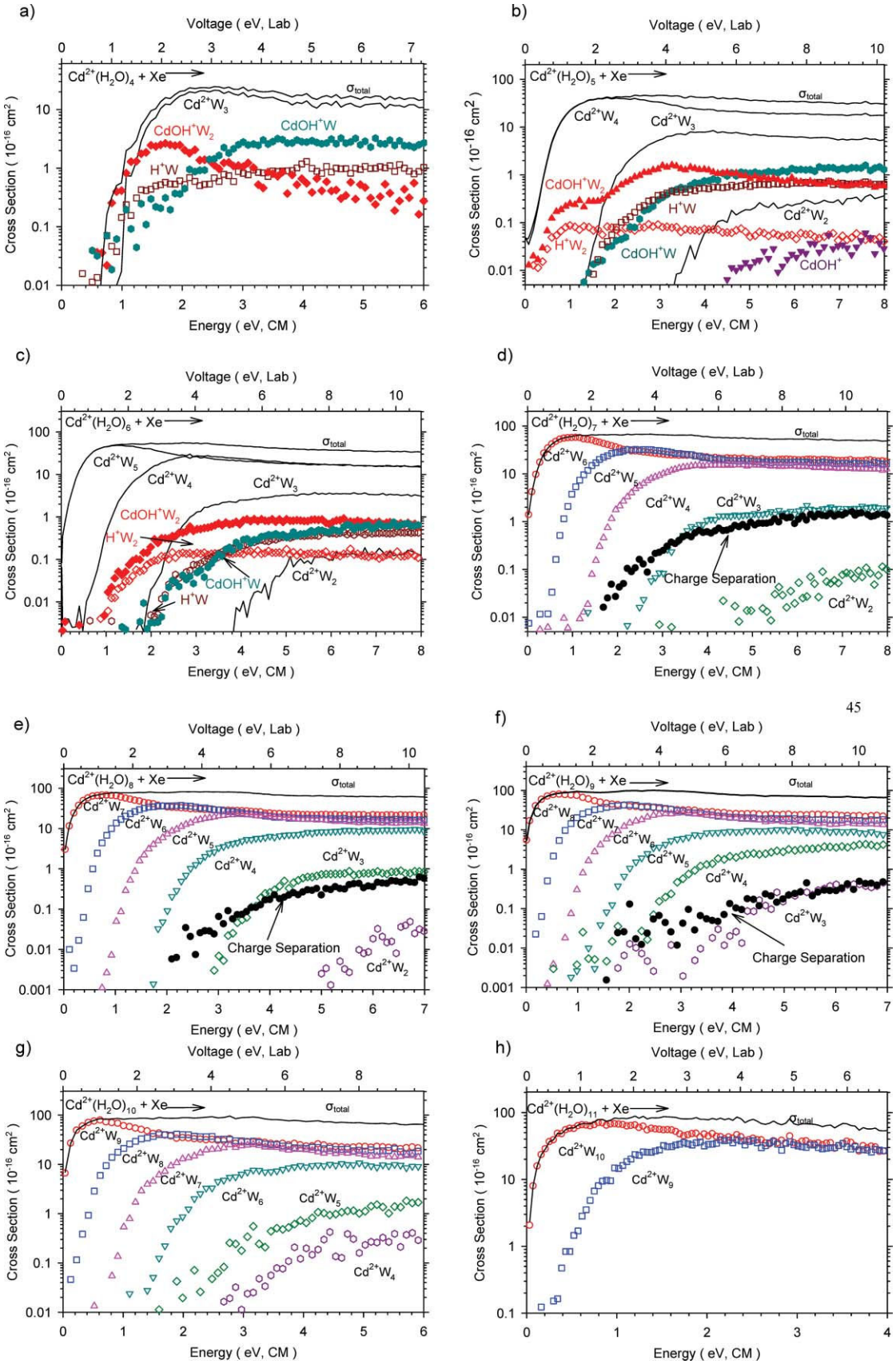

FIG. 1. CID cross sections for the sequential water loss (lines in parts a–c and open symbols in parts d–h) and charge separation processes (symbols in parts a–c and solid symbols in parts d–h) for $Cd^{2+}W_n$, where $n = 4$–11 and W = H_2O colliding with Xe at 0.2 mTorr as a function of laboratory voltage (upper x-axis) and center-of-mass energy (lower x-axis).

$CdOH^+(H_2O)_2$ product, while $H^+(H_2O)$ is formed in both reactions (3) and (4). These trends and pathways are discussed further below in the context of the available thermochemistry.

Although the relative magnitudes of the product cross sections shown in Fig. 1(a) provide good qualitative information, the absolute magnitudes of these products may be inaccurate because the $^{114}Cd^{2+}(H_2O)_4$ reactant has the same mass as $K^+(H_2O)_3$, a common contaminant in these solutions. This is also the reason why no $Cd^{2+}(H_2O)_2$ product is shown in Fig. 1(a), as this product has the same mass as a $K^+(H_2O)_2$ product. Utilization of other isotopes of Cd^{2+} were equally problematic because the other main isotopes of Cd have mass overlaps with other common contaminant ions found in our instrument: $Ca^{2+}(H_2O)_8$ and $H^+(H_2O)_5$. Studies using different metals hydrated with D_2O have been attempted, but the intensities of pure $M^{2+}(D_2O)_n$ complexes formed in our source are not sufficient to conduct threshold collision-induced dissociation experiments. It should be noted that this contamination problem does not affect the thermochemical and threshold information derived from the primary water loss or charge separation products of the dissociation of $n = 4$. It only affects the absolute values of the cross sections and therefore the $\sigma_{0,j}$ values used in the modeling. No other $Cd^{2+}(H_2O)_n$ complexes had similar difficulties.

C. $n = 5$

In the dissociation of $Cd^{2+}(H_2O)_5$, products are observed for reactions (1) and (5), Fig. 1(b).

$$Cd^{2+}(H_2O)_5 + Xe \rightarrow CdOH^+(H_2O)_2 + H^+(H_2O)_2 + Xe. \quad (5)$$

Both products formed in reaction (5) have a higher apparent threshold than the water loss product from reaction (1) indicating that reaction (1) is energetically favored over reaction (5). Products of reaction (5) have a much smaller cross section than the $Cd^{2+}(H_2O)_4$ product (by over 2 orders of magnitude) because reaction (5) is both thermodynamically and entropically disfavored over reaction (1). Reaction (3) is also observed in the sequential dissociation of $Cd^{2+}(H_2O)_5$, as evidenced by the increase in magnitude of the $CdOH^+(H_2O)_2$ cross section above ~1.4 eV. Further, this second feature is not observed in the $H^+(H_2O)_2$ product cross section, but does match the appearance of the $H^+(H_2O)$ product associated with reaction (3). As shown in Fig. 1(a), the threshold for reaction (3) [as exhibited by both the second feature of $CdOH^+(H_2O)_2$ and the onset of $H^+(H_2O)$] appears close to but slightly below that for formation of $Cd^{2+}(H_2O)_3$. Examination of the $CdOH^+(H_2O)$ cross section also shows two features, both of which start at ~1 eV above the more obvious onsets in the $CdOH^+(H_2O)_2$ cross section. In both cases, the $CdOH^+(H_2O)$ product is probably formed by water loss from the $CdOH^+(H_2O)_2$ product formed in reactions (3) and (5), but could also have contributions from reaction (4) at higher energies, as discussed below in further detail.

D. $n = 6$

The dominant reaction observed in the dissociation of $Cd^{2+}(H_2O)_6$ is the loss of a single water molecule, followed by the sequential loss of additional water molecules as the collision energy increases down to $n_{min} = 2$. For $n = 6$, no additional charge separation products were observed other than those already discussed for the smaller complexes, Fig. 1(c). Thus reaction (2) is higher in energy than both reaction (1) and the sequential loss of another water ligand to form $Cd^{2+}(H_2O)_4$, consistent with the discussions above and Fig. 1(b). Above about 2 eV, the $CdOH^+(H_2O)_2$ product continues to increase in magnitude while the $H^+(H_2O)_2$ product cross section levels and then begins to gradually decrease above 3 eV, most likely corresponding to a water loss dissociation. As shown in Fig. 1(b), the additional increase in the $CdOH^+(H_2O)_2$ product cross section matches the appearance of the $H^+(H_2O)$ product indicating the onset of reaction (3). Unlike Figs. 1(a) and 1(b), the products of reaction (3) appear to have a higher apparent threshold than that for the formation of $Cd^{2+}(H_2O)_3$, but because these ion intensities are now all much smaller, this is simply an issue of sensitivity. As shown in Fig. 1(b), the $CdOH^+(H_2O)$ cross section exhibits two features that probably correspond to water loss dissociation from the $CdOH^+(H_2O)_2$ products formed in reactions (3) and (5) with possible contributions from reaction (4).

E. $n = 7$–11

In all cases, the dominant reactions are the loss of a single water molecule, reaction (1), followed by the loss of additional water molecules as the collision energy increases, Figs. 1(d)–1(h). This behavior has been discussed previously.[17] For these five systems, the charge separation reactions observed do not complicate the dissociation of the first two water ligands. The $Cd^{2+}(H_2O)_{11}$ reactant was observed with very small intensity such that data for loss of only the first two water ligands were collected, Fig. 1(h), although loss of three waters was observed experimentally.

As mentioned above, the smallest cadmium water complex observed is $Cd^{2+}(H_2O)_2$, Figs. 1(b)–1(e). $Cd^{2+}(H_2O)_3$ and $Cd^{2+}(H_2O)_2$ product cross sections are considerably smaller than that of the $Cd^{2+}(H_2O)_4$ product by factors of about 2 and 60 at elevated collision energies in Fig. 1(b) (and even larger factors for larger parent complexes). In addition, the energy gaps between the onsets of $Cd^{2+}(H_2O)_4$, $Cd^{2+}(H_2O)_3$, and $Cd^{2+}(H_2O)_2$ are considerably larger than between any other pair of sequential products. These observations parallel those found in our hydration studies of Zn^{2+} ($n_{min} = 3$) (Ref. 26) but are distinct from those found for Ca^{2+} and Sr^{2+} ($n_{min} = 0$).[59,60] For all four metal dications, the general trends are explained by gradually increasing hydration energies as n decreases, and this explanation is sufficient for Ca^{2+} and Sr^{2+}. For both Zn^{2+} and Cd^{2+}, another possible contribution comes from the enhanced stability given by the $18e^-$ rule, as fulfilled for their $n = 4$ complexes, and discussed further below. Another contributing factor to the substantial decrease in the magnitude of the $Cd^{2+}(H_2O)_2$ cross section comes from the energetic preference for the charge

TABLE I. Relative calculated enthalpies (ΔH_0) and free energies (ΔG_{298})[a] in kJ/mol of $Cd^{2+}(H_2O)_n$.

		SD/6-311+G(2d,2p)		Def2TZVPP	
n	Complex name	B3LYP[b]	MP2(full)[b]	B3LYP[c]	MP2(full)[c]
5	(5,0)	0.0 (0.0)	0.0 (0.0)	0.0 (0.0)	0.0 (0.0)
	(4,1)_A	11.1 (4.8)	26.2 (20.0)	9.9 (4.9)	18.6 (13.6)
6	(6,0)	0.0 (1.4)	0.0 (0.0)	0.0 (0.0)	0.0 (0.0)
	(5,1)_A_bA_b	3.7 (1.0)	17.1 (13.1)	3.0 (0.6)	11.0 (8.6)
	(5,1)_A_a	10.7 (0.0)	26.8 (14.7)	10.0 (0.6)	19.5 (10.1)
	(4,2)_2AA	9.8 (15.8)	35.0 (39.6)	8.1 (13.7)	22.8 (28.4)
7	(6,1)_AA	4.8 (1.0)	0.0 (0.0)	7.1 (2.8)	0.0 (0.0)
	(5,2)_2A_bA_b	0.0 (1.6)	8.4 (13.8)	0.0 (0.9)	0.7 (5.9)
	(5,2)_A_bA_b,A_a	7.1 (0.0)	18.4 (15.1)	7.5 (0.0)	9.9 (6.8)
	(4,3)_4D_AA,2A	15.5 (3.6)	41.7 (33.6)	14.8 (3.1)	26.5 (19.2)
	(7,0)	39.8 (31.8)	22.4 (18.2)	42.9 (35.5)	26.3 (23.3)
8	(6,2)_4D_2AA	2.9 (1.2)	0.0 (0.0)	5.6 (5.0)	0.0 (3.1)
	(6,2)_2D,DD_2AA	3.8 (4.0)	0.9 (2.7)	10.1 (1.5)	4.9 (0.0)
	(5,3)_2A_bA_b,A_aA_b	0.0 (2.2)	11.8 (15.6)	0.0 (0.4)	3.3 (7.5)
	(5,3)_3A_bA_b	2.3 (2.2)	13.7 (15.3)	2.4 (0.0)	5.3 (6.7)
	(5,3)_2A_bA_b,A_b	5.7 (0.0)	19.8 (15.7)	6.3 (0.2)	11.6 (9.3)
	(4,4)_2AA,2A	15.4 (9.4)	43.6 (39.3)	14.2 (6.1)	27.6 (23.2)
9	(6,3)_6D_3AA	0.0 (4.5)	0.0 (4.0)	0.0 (8.9)	0.0 (4.8)
	(6,3)_4D,DD_3AA	2.8 (1.0)	2.4 (0.0)	2.9 (4.4)	2.6 (0.0)
	(5,4)_3A_bA_b,A_a	7.3 (0.2)	23.5 (15.8)	6.1 (3.3)	16.5 (9.6)
	(4,5)_AA,4A	25.0 (0.0)	61.1 (35.6)	22.0 (0.0)	44.7 (18.7)
10	(6,4)_4AA	0.0 (5.6)	0.0 (0.3)	0.0 (4.8)	0.0 (0.0)
	(6,4)_3AA,A	3.0 (4.2)	4.1 (0.0)	3.7 (7.1)	3.9 (2.5)
	(6,4)_2AA,AAD,A_1A_2	4.5 (12.5)	2.8 (5.5)	5.5 (15.4)	3.9 (8.9)
	(5,5)_4A_bA_b,A_a	0.8 (0.0)	17.3 (11.2)	0.0 (0.0)	9.5 (4.6)
	(4,6)_2AA,4A	17.1 (7.6)	51.2 (36.4)	14.0 (1.8)	35.3 (18.3)
11	(6,5)_3AA,AAD,A_1A_2	0.0 (13.3)	0.0 (6.5)	0.5 (16.8)	0.0 (6.4)
	(6,5)_4AA,A	3.5 (5.5)	4.8 (0.0)	3.5 (9.1)	4.4 (0.0)
	(5,5,1)_3A_bA_b,A_a,A_bA_bD_A	2.2 (0.0)	23.0 (16.7)	0.0 (0.0)[d]	12.9 (3.1)[d]
	(7,4)_4AA	28.9 (40.3)	19.9 (24.4)	30.9 (44.9)	23.1 (27.2)

[a]ΔG_{298} values given in parenthesis.
[b]Single point energies calculated at each respective level shown using a SD/6-311+G(2d,2p) basis set with geometries calculated at B3LYP/SD/6-311+G(d,p). ZPE correction included.
[c]Single point energies calculated at each respective level shown using a Def2TZVPP basis set with geometries calculated at B3LYP/Def2TZVP. ZPE correction included.
[d]Structure converged but not in conjunction with frequency calculation.

separation reaction (4) versus reaction (1) for the dissociation of $n = 3$. At high energies, the $CdOH^+(H_2O) + H_3O^+$ product channel has a larger magnitude than the entropically favored $Cd^{2+}(H_2O)_2 + H_2O$ product channel, in contrast to observations for reactions (3) and (5) versus reaction (1) for $n = 4$ and 5, respectively. The relative energetics are discussed more quantitatively below. Of course, such minimum sizes have been reported previously for $Cd^{2+}(H_2O)_n$ as $n_{min} = 1$ (Ref. 9) and ≤ 7 (Ref. 10); however, such comparisons are not very useful as the minimum size observed is very dependent on instrumental sensitivity, source conditions, and collision conditions.

F. Theoretical geometries: $Cd^{2+}(H_2O)_n$

Our previous work[17] gave a detailed discussion of the predicted GS structures at the MP2(full) level for $n = 1$–11 complexes, as well as comparisons between previously reported structures[25,61] of $Cd^{2+}(H_2O)_n$ and the respective complexes of Zn^{2+} and Ca^{2+}. Since that report, further calculations were performed to ensure that all structures are fully converged after the frequency calculation leading to relative energies and vibrational frequencies that have changed slightly (relative energies by <2 kJ/mol and frequencies by <10%,). Relative 0 K enthalpies and 298 K free energies for the low-energy isomers of different inner shell sizes are presented in Table I for results calculated using both the SD/6-311+G(2d,2p) and Def2TZVPP basis sets at the B3LYP and MP2(full) levels. Similar calculations using the B3P86 level of theory were also performed, yielding results close to those of the B3LYP level and therefore are given in the supporting information section, Table S1.

Our (x, y, z) nomenclature describes the different conformations of $Cd^{2+}(H_2O)_x(H_2O)_y(H_2O)_z$, where x, y, and z are the number of water molecules in the first, second, and third shells, respectively. When needed, this designation is

augmented by the hydrogen bonding motif of the isomer, where a second shell water molecule that hydrogen bonds to two different inner shell water molecules is a double acceptor (AA), whereas a second shell water molecule that forms only one hydrogen bond to the inner shell is a single acceptor (A). An inner shell water molecule that donates either one or two hydrogen bonds is designated as a single or double donor (D or DD, respectively). Water molecules in the second shell that hydrogen bond to water molecules in the third shell are a combination of both an acceptor and donor water molecule and are named accordingly.

A number of additional higher energy isomers were also calculated for all inner shell sizes of the $n = 5$–11 complexes. Because of the large number of high and low-energy isomers investigated using the two different basis sets, their relative energetics and structures are given in the supporting information section, Table S1 and Figure S1.[62] In general, trends in the relative energetics for both basis sets are in agreement with each other, although specific complexes where results disagree are discussed below.

For $n = 1$–5, all levels of theory predict that the lowest-energy conformers at both 0 and 298 K have all water ligands coordinating directly to the metal ion through the oxygen atom, as previously discussed.[17] For $n = 6$, the 0 K GS is the (6,0) structure at each level of theory and at 298 K for MP2(full) and B3LYP/Def2TZVPP calculations; whereas, B3LYP/SD/6-311+G(2d,2p) calculations find that the (6,0) complex is within 1 kJ/mol of a (5,1)_A_a GS complex (where the A_a designation indicates that the sixth water is singly hydrogen bound to the apex water in a square pyramid inner shell). The (5,1)_A_bA_b complex is also low in energy at the DFT levels, where the second shell water forms two hydrogen bonds with the base of the square pyramidal inner shell, as designated by the A_b nomenclature. For $n = 7$, low energy structures include (6,1)_AA [the MP2(full) GS at 0 and 298 K], (5,2)_2A_bA_b (the DFT GS at 0 K), and (5,2)_A_bA_b,A_a (the DFT GS at 298 K). This latter structure has one A water molecule forming a single hydrogen bond to the inner shell thereby making a weaker bond compared to an AA water, but such an arrangement is entropically favored over the (5,2)_2A_bA_b because of the near free rotation allowed for the A water.

For $n = 8$, the MP2(full)/SD/6-311+G(2d,2p) GS is the (6,2)_4D_2AA complex at both 0 and 298 K, whereas, the (6,2)_2D,DD_2AA complex is 1–3 kJ/mol higher in energy, Fig. 2. Interestingly, at the MP2(full)/Def2TZVPP level, the (6,2)_2D,DD_2AA complex is the free energy GS by 3 kJ/mol but higher in 0 K enthalpy ($\Delta\Delta H_0 = 5$ kJ/mol). Clearly these two complexes are isoenergetic with each other at the MP2(full) level. The DFT relative energies for these (6,2) complexes are higher in energy by 1–5 kJ/mol in 298 K free energy ($\Delta\Delta H_0 = 3$–10 kJ/mol) over five-coordinate complexes using either basis set. These DFT levels predict the 0 K GS to be (5,3)_2A_bA_b,A_aA_b; however, this complex has essentially the same (within 2 kJ/mol) 298 K free energy as the (5,3)_2A_bA_b,A_b and (5,3)_3A_bA_b complexes. All five-coordinate complexes are higher in 298 K free energy than the six-coordinate GS by 7–16 kJ/mol at the MP2(full) level. The (4,4)_2AA,2A complex is higher in 298 K free energy by 6–9 kJ/mol at the DFT levels and 23–39 kJ/mol at the MP2(full) level.

For $n = 9$ and 10, the 0 K GSs are the (6,3)_6D_3AA and (6,4)_4AA complexes at all levels of theory. At 298 K, MP2(full) calculations find that the (6,3)_4D,DD_3AA complex is favored by 4 kJ/mol using either basis set and for $n = 10$, find two low-energy complexes at 298 K, (6,4)_4AA and (6,4)_3AA,A, which lie within 4 kJ/mol of one another at 0 and 298 K. In contrast, DFT calculations find that the 6-coodinate species are higher in free energy for both $n = 9$ and 10. For $n = 9$, the (4,5)_AA,4A complex is the 298 K GS using either basis set, but is higher in 0 K enthalpy ($\Delta\Delta H_0 = 22$–25 kJ/mol). Close in free energy to the (4,5) complex is the (5,4)_3A_bA_b,A_a, similar to (5,5)_4A_bA_b,A_a, the DFT free energy GS structure for $n = 10$ found with both basis sets.

For $n = 11$, the 0 K GS complex at the B3LYP/SD/6-311+G(2d,2p) and both MP2(full) levels is the (6,5)_3AA,AAD,A_1A_2 complex, where one double acceptor water hydrogen bonds to both the first and second solvent shell (A_1A_2) thereby forming a ringlike series of hydrogen bonds (which we have previously called AA_p because a pseudo third solvent shell is formed). Thus, there is also a second shell water that is both a double acceptor and donor water molecule (AAD). At 298 K, the (6,5)_4AA,A free energy GS complex is lower by 6–7 kJ/mol at the MP2(full) level using either basis set; however, this complex is 6–9 kJ/mol higher in free energy than the (5,5,1)_3AA,A,AAD_A structure at the DFT levels (although this structure could not be fully converged using the Def2TZVP basis set because of large motions and displacements of the single acceptor waters). No four-coordinate structures were calculated at this complex size. The (7,4)_4AA complex is higher in energy at all levels by 20–45 kJ/mol.

G. Comparison to $Zn^{2+}(H_2O)_n$

The conflicting theoretical results on the predicted low-energy structures between the DFT and MP2(full) levels are similar to our recent investigation of zinc hydration.[26] In the case of hydrated zinc, the DFT levels favored four-coordinate complexes as the GSs, with five and six-coordinate complexes higher in 298 K free energy by 1–12 kJ/mol and 7–36 kJ/mol, respectively, for $n = 6$–10. In contrast, the MP2(full) level of theory favored five-coordinate complexes over both four and six-coordinate structures by 2–8 kJ/mol and 4–16 kJ/mol, respectively. The M06 functional,[63,64] which is specifically designed to handle hydrogen bonding, gave similar relative energies as those predicted by the MP2(full) level. The experimental bond dissociation energies for water loss from the $n = 6$ to 10 complexes were reproduced by an average of 2 kJ/mol better using the structures and energies predicted by the MP2(full) level of theory over the B3LYP and B3P86 levels. (Calculations using the M06 functional were in poor agreement with experiment.[26]) Although a 2 kJ/mol difference is hardly conclusive, this observation suggests that the GS structure of gas phase hydrated Zn^{2+} is five-coordinate and that the MP2(full) level is more accurate than B3LYP and

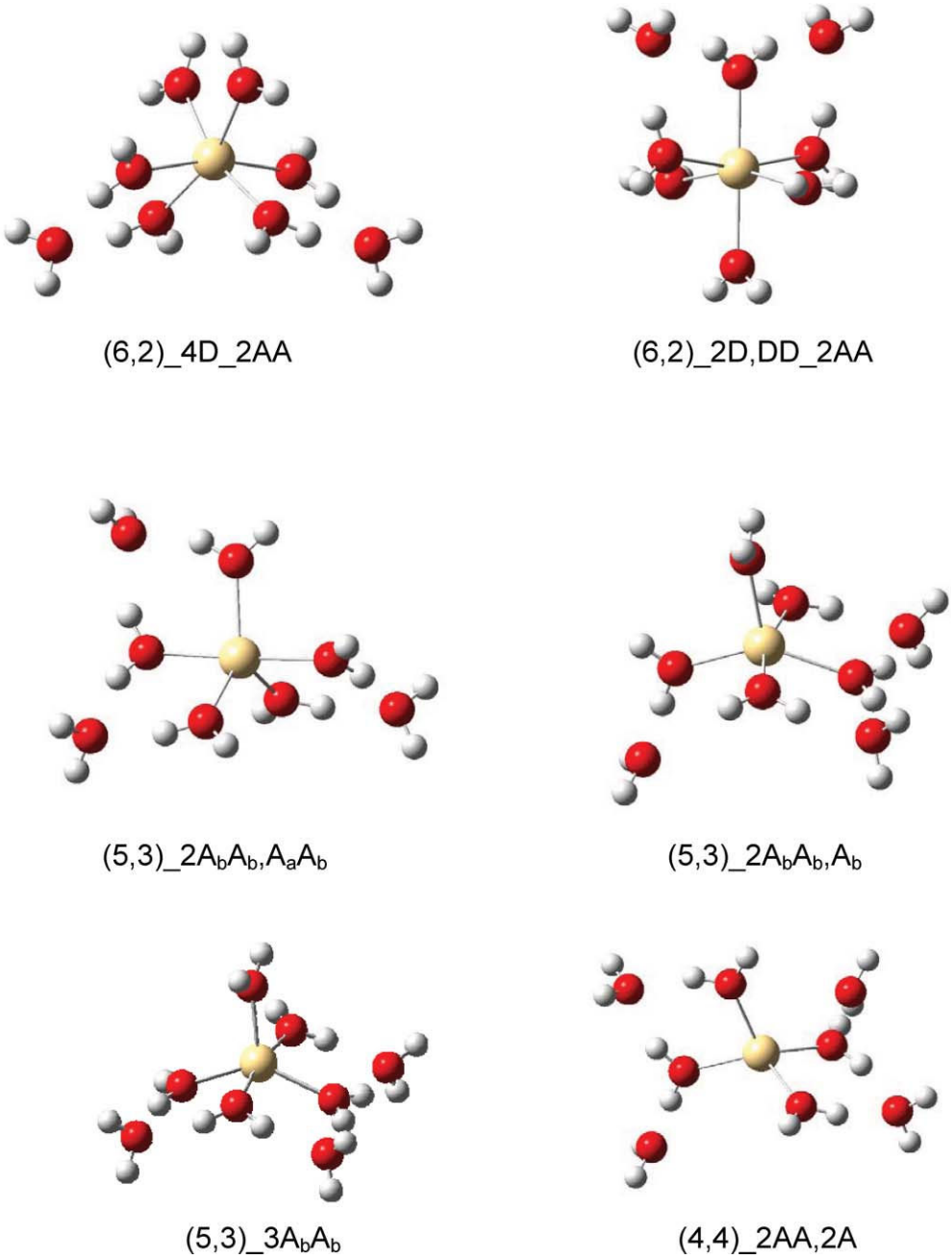

FIG. 2. Low-energy isomers of $Cd^{2+}(H_2O)_8$ calculated at the B3LYP/SD/6-311+G(d,p) level of theory.

B3P86 for these systems. This conclusion was recently confirmed by infrared photodissociation spectroscopic studies,[34] which show a preference for a coordination number of 5 with possible contributions from 6. No evidence consistent with four-coordinate species was observed. A key conclusion of this spectroscopy study was that B3LYP and B3P86 relative energies do not appear to be reliable for these hydrated complexes, therefore, the MP2(full) predicted low-energy complexes of $Cd^{2+}(H_2O)_n$ will be used in the analysis of our experimental data.

The results of the MP2(full) calculations predict that the low-energy structures of hydrated Cd^{2+} have an inner shell of six, one water molecule larger than those predicted for hydrated Zn^{2+}. This difference is a consequence of the larger ionic radius of Cd^{2+} versus that of Zn^{2+}, 0.99 and 0.78 Å,[65] respectively, and the higher nuclear charge of the Cd^{2+} ion.

H. Theoretical geometries: charge separation transition states

The rate-limiting step of reaction (2) is needed for the thermochemical analysis of this dissociation and involves the $H^+(H_2O)_{n-m-1}$ pulling away from the complex leaving $CdOH^+(H_2O)_m$, where $m = 3$ for $n = 6$, $m = 2$ for $n = 5$ and 4, and $m = 1$ for $n = 3$. The optimized tight TSs of the charge separation processes occurring for $n = 3$–6 are shown in Fig. 3. In all cases, both the $CdOH^+(H_2O)_m$ and $H^+(H_2O)_{n-m-1}$ portions of each TS have geometries

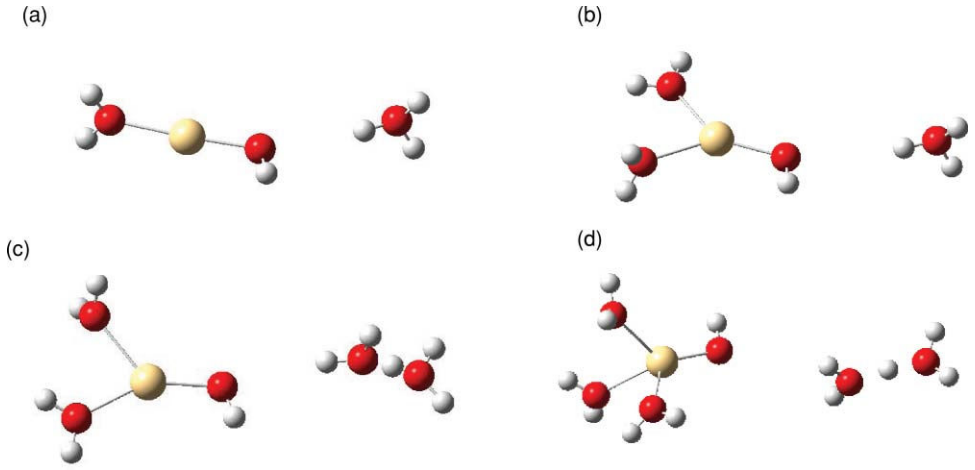

FIG. 3. Optimized rate-limiting transition states of the $n = 3$, 4, 5, and 6 charge separation products $CdOH^+(H_2O)_m + H^+(H_2O)_{n-m-1}$, where $m = 1$, 2, 2, and 3 and $n - m - 1 = 1$, 1, 2, and 2 for parts a–d, respectively, calculated at the B3LYP/Def2TZVP level of theory.

similar to their respective GS products. Although complete reaction coordinate diagrams were not calculated for these charge separation reactions, the TSs shown correspond to the Coulomb barrier associated with the approach of the two singly charged product ions, which must be the rate-limiting TS along the reaction coordinate. This was explicitly shown to be the case for the charge separation of $Zn^{2+}(H_2O)_7$ where the complete reaction coordinate was calculated.[49] The barrier heights of these processes will be discussed in quantitative detail below.

I. Thermochemical results

Cross sections for the primary and secondary dissociation products were analyzed in several ways, with Table II summarizing the average optimum modeling parameters. Threshold E_0 values are given for the primary dissociation of each complex from modeling a single dissociation channel and including lifetime effects. If lifetime effects are not included, the threshold obtained from analysis is higher because of a kinetic shift. The kinetic shifts and primary threshold values have been discussed elsewhere for this system.[17] The vibrational frequencies calculated at the B3LYP/SD/6-311+G(d,p) level were used in the RRKM analysis presented here, although it was verified that the optimum modeling parameters do not change outside of the listed uncertainties when frequencies calculated at the B3LYP/Def2TZVP level are used instead. Additionally, the primary threshold energies obtained were not affected by any changes in the vibrational frequencies resulting from the additional calculations taken to ensure structural convergence, Table II. However, these new calculations did lead to slight changes in the relative energies of a couple low-energy isomers, such that the experimental data for the $n = 8$ and 10 complexes were also interpreted assuming two additional structures. For $n = 10$, MP2(full)/SD/6-311+G(2d,2p) calculations indicate that the (6,4)_3AA,A isomer is in thermal equilibrium with the (6,4)_4AA reactant and may dissociate to the (6,3)_6D_3AA complex. Assuming that the $n = 10$ reactant complex is (6,4)_3AA,A instead of (6,4)_4AA lowers the threshold by 0.05 eV to 0.44 ± 0.05 eV because of a change in the kinetic shift. Similar changes in kinetic shifts are discussed in detail in our previous zinc hydration study.[26] Briefly, if the assumed reactant complex has more outer shell waters with lower torsional frequencies (i.e., more single acceptor water molecules), it has a higher density of states, which lowers the rates of dissociation. This in turn increases the kinetic shift thereby lowering the 0 K threshold, as seen for the (6,4)_3AA,A reactant. For $n = 8$, the (6,2)_2D,DD_2AA primary dissociation to (6,1)_AA is now included because the MP2(full)/Def2TZVPP level predicts this reactant complex to be the 298 K free energy GS as opposed to the (6,2)_4D_2AA complex predicted by the MP2(full)/SD/6-311+G(2d,2p) level. Here, there is a negligible change to the threshold (a difference of 0.01 eV) because of the similarities in the hydrogen bonding network of these two complexes.

J. Competitive analysis: water loss versus charge separation

The dissociation pathways of $Cd^{2+}(H_2O)_4$ and $Cd^{2+}(H_2O)_5$ are both influenced by the competition between the water loss and charge separation processes. For competing channels, the thermodynamically favored reaction pathway will remain largely unaffected, but the threshold of the disfavored pathway will shift to lower energies once competition is accounted for, known as a competitive shift. (Note that the uncertainty in the relative thresholds for competing channels is typically lower than the combined absolute uncertainties for each individual channel because several contributions to the uncertainty cancel in the relative value.) For reasons discussed previously in our study of charge separation in the zinc system,[49] the lowest five vibration frequencies of the tight TSs were changed to rotational degrees of freedom in our threshold analysis for $n = 4$ and 5 to better reproduce the energy dependence of the experimental cross sections of the charge separation products. For each of these TSs, one vibrational frequency corresponds to a torsion of the complex about the reaction coordinate and the other four vibrations are rotations of each incipient product, $CdOH^+(H_2O)_m$ and $H^+(H_2O)_{n-m-1}$.

TABLE II. Optimized parameters from analysis of CID cross sections[a].

n	Reactant	Product	$\sigma_{0,j}$	N	$E_{0,j}$ (eV)	$\Delta S^{\dagger}_{1000}$ (J/mol K)
4	(4,0)	(3,0)[b]	52 (3)	0.6 (0.1)	1.61 (0.05)	25 (5)
	(4,0)	TS[2 + 1][b]	5 (1)	0.4 (0.1)	1.34 (0.04)	29 (5)
	(4,0)	(3,0)[c]	48 (3)	0.8 (0.1)	1.52 (0.04)	20 (5)
		TS[2 + 1][c]	0.03 (0.03)	0.8 (0.1)	1.31 (0.03)	29 (5)
5	(5,0)	(4,0)[b]	70 (4)	0.8 (0.1)	1.11 (0.05)	60 (5)
	(5,0)	(4,0)[d]	72 (4)	0.8 (0.1)	1.11(0.05)	60 (5)
		(3,0)[d]	29 (4)	0.8 (0.1)	2.73 (0.05)	
	(5,0)	TS[2 + 2][b]	2 (2)	0.1 (0.2)	1.21 (0.07)	39 (5)
	(5,0)	(4,0)[c]	68 (7)	0.8 (0.2)	1.10 (0.03)	60 (8)
		TS[2 + 2][c]	0.1 (0.2)	0.8 (0.2)	1.14 (0.03)	39 (5)
	(5,0)	(3,0)[e]	39 (11)	0.2 (0.1)	2.72 (0.11)	22 (5)
		(2,0)[e]	1 (0.5)	0.2 (0.1)	4.85 (0.18)	
6	(6,0)	(5,0)[b]	64 (4)	0.9 (0.1)	0.90 (0.05)	56 (5)
	(6,0)	(5,0)[d]	65 (3)	0.9 (0.1)	0.90 (0.04)	56 (5)
		(4,0)[d]	60 (20)	0.9 (0.1)	2.10 (0.05)	
	(6,0)	(4,0)[e]	60 (12)	0.7 (0.2)	1.97 (0.08)	57 (5)
		(3,0)[e]	11 (3)	0.7 (0.2)	3.75 (0.20)	
7	(6,1)	(6,0)[b]	80 (4)	0.8 (0.1)	0.70 (0.05)	39 (4)
	(6,1)	(6,0)[d]	77 (5)	0.9 (0.1)	0.67 (0.05)	41 (4)
		(5,0)[d]	78 (12)	0.9 (0.1)	1.67 (0.07)	
8	(6,2)	(6,1)[b]	96 (5)	0.8 (0.1)	0.66 (0.06)	63 (5)
	(6,2)	(6,1)[d]	88 (5)	0.9 (0.1)	0.62 (0.08)	63 (4)
		(6,0)[d]	75 (7)	0.9 (0.1)	1.37 (0.09)	
	(6,2)_2D,DD_2AA	(6,1)[b]	95 (5)	0.8 (0.1)	0.67 (0.06)	69 (5)
9	(6,3)_4D,DD_3AA	(6,2)[b]	109 (2)	0.8 (0.1)	0.61 (0.05)	59 (5)
	(6,3)_4D,DD_3AA	(6,2)[d]	103 (3)	0.7 (0.1)	0.62 (0.06)	59 (4)
		(6,1)[d]	70 (11)	0.7 (0.1)	1.34 (0.08)	
10	(6,4)	(6,3)[b]	95 (6)	0.9 (0.1)	0.49 (0.05)	18 (5)
	(6,4)	(6,3)[d]	91 (2)	0.9 (0.1)	0.45 (0.06)	19 (4)
		(6,2)[d]	75 (5)	0.9 (0.1)	1.16 (0.07)	
	(6,4)_3AA,A	(6,3)[b]	91 (2)	0.9 (0.1)	0.44 (0.05)	9 (5)
11	(6,5)_4AA,A	(6,4)[b]	59 (4)	1.1 (0.1)	0.43 (0.05)	23 (4)
	(6,5)_4AA,A	(6,4)[d]	59 (4)	1.1 (0.1)	0.41 (0.06)	23 (5)
		(6,3)[d]	37 (5)	1.1 (0.1)	1.06 (0.09)	

[a]Uncertainties in parentheses.
[b]Single channel dissociation model.
[c]Competitive dissociation model.
[d]Sequential dissociation model.
[e]Tertiary fit using the sequential dissociation model.

Figure 4 shows a representative model for the competitive dissociation of $Cd^{2+}(H_2O)_4$. The rate limiting TSs for reaction (2) are abbreviated according to the products formed, i.e., TS[$m + (n - m - 1)$]. For $n = 4$, the thermodynamically favored TS[2 + 1] has a threshold of 1.31–1.34 eV whether the cross section is fit independently or with competition; whereas the water loss channel shifts down from 1.61 ± 0.05 to 1.52 ± 0.04 eV, a competitive shift of 0.09 ± 0.03 eV, Table II. The charge separation dissociation pathway is favored by 0.18–0.21 ± 0.03 eV over the water loss channel. A similar competitive shift of 0.08 eV for the analogous water loss dissociation channel was seen in the zinc hydration study, which favored the charge separation channel by 0.13 eV for the dissociation of $Zn^{2+}(H_2O)_7$.[49]

The water loss threshold for $n = 5$ remains between 1.10 and 1.11 eV regardless of how this cross section is analyzed, Table II. However, the threshold for charge separation at $n = 5$, TS[2 + 2], is 1.14 ± 0.03 eV and shifts up by 0.07 ± 0.04 eV if competition is not included. This competitive shift is smaller than that for the analogous charge separation dissociation of $Zn^{2+}(H_2O)_8$ (also the thermodynamically disfavored pathway) of 0.16 eV.[49] The competitive shift seen for the $Cd^{2+}(H_2O)_5$ system is probably smaller because of the proximity in the thresholds for the water loss and charge separation pathways, which only differ by 0.03–0.04 ± 0.03 eV in favor of the water loss channel, compared to the $Zn^{2+}(H_2O)_8$ system, where the water loss pathway is favored by 0.07–0.09 eV.

K. Water loss secondary threshold energies

There is no primary charge separation process to complicate the dissociation of $Cd^{2+}(H_2O)_n$, where n = 6–11,

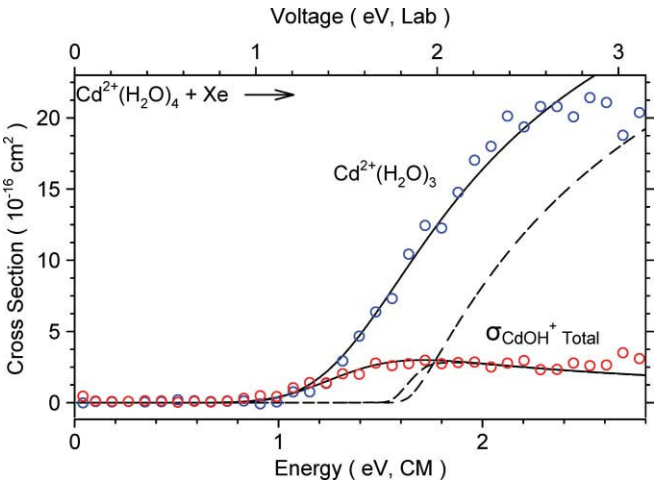

FIG. 4. Cross sections for the CID of $Cd^{2+}(H_2O)_4$ with 0.15 mTorr of Xe. Solid lines show the best fit to the primary water loss and the competing charge separation product ion using the primary model convoluted over the kinetic and internal energy distributions of the neutral and ionic reactants. Dashed lines show the models in the absence of experimental kinetic energy broadening for reactants with an internal energy of 0 K. Optimized parameters for this model are found in Table II.

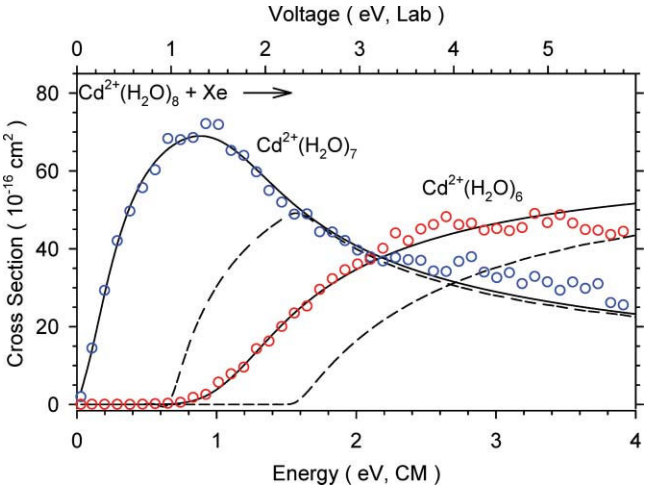

FIG. 5. Zero pressure extrapolated cross sections for the CID of $Cd^{2+}(H_2O)_8$ with Xe. Solid lines show the best fit to both the primary and secondary water loss products using the sequential model convoluted over the kinetic and internal energy distributions of the neutral and ionic reactants. Dashed lines show the models in the absence of experimental kinetic energy broadening for reactants with an internal energy of 0 K. Optimized parameters for this model are found in Table II.

therefore, the secondary water loss was analyzed using a sequential model with equations described elsewhere,[40,48] and the results are reported in Table II. In modeling the secondary (and primary) dissociation, the reactant isomer is assumed to be the 298 K GS (as this species should have the dominant population in a thermally equilibrated source) and the product isomer is the 0 K GS (as our threshold analysis is dominated by the lowest 0 K enthalpy species), which goes on to dissociate to the 0 K GS secondary product isomer.[26] As for competing channels, the uncertainty in the "sequential BDE," which is derived from the difference between the primary and secondary thresholds, is typically lower than the calculated absolute uncertainty for primary and secondary thresholds because several contributions to the uncertainty in the energy cancel in the relative value. A representative model is shown in Fig. 5 for the sequential dissociation of $Cd^{2+}(H_2O)_8$ assumed to be a (6,2)_4D_2AA reactant dissociating to (6,1) + H_2O and (6,0) + $2H_2O$. From this point forward, we abbreviate our naming scheme to (*x*,*y*) for the lowest energy isomer of each inner solvent shell, except for instances where the ΔG_{298} and ΔH_0 complexes differ at the MP2(full)/SD/6-311+G(2d,2p) level, where the full name of the ΔG_{298} GS is given. In cases where the GS differs between the two basis sets, the full name of the GS predicted by the Def2TZVPP basis set is given.

For the sequential dissociation of $Cd^{2+}(H_2O)_{11}$, modeled as (6,5)_4AA,A → (6,4) + H_2O → (6,3) + $2H_2O$, the sequential BDE for the dissociation energy of $Cd^{2+}(H_2O)_9$-H_2O is 0.65 ± 0.07 eV. This result is 0.16 ± 0.09 eV higher in energy than the primary water loss threshold of 0.49 ± 0.05 eV for $n = 10$ when modeled as a (6,4) → (6,3) + H_2O process. This difference will be discussed further below.

The secondary threshold for $n = 10$ is 1.16 ± 0.07 eV, modeled as (6,4) → (6,3) + H_2O → (6,2) + $2H_2O$, yielding a primary–secondary threshold difference of 0.71 ± 0.05 eV for $Cd^{2+}(H_2O)_8$-H_2O. This sequential BDE is 0.10 ± 0.08 eV higher than the primary dissociation threshold for $n = 9$. For $n = 9$, the sequential model gives a relative threshold value of 0.72 ± 0.03 eV for $Cd^{2+}(H_2O)_7$-H_2O, as modeled assuming a (6,3)_4D,DD_3AA → (6,2) + H_2O → (6,1) + $2H_2O$ process, only 0.06 ± 0.07 eV higher than the primary dissociation threshold for $n = 8$, within experimental uncertainty. For n = 6–8, the primary–secondary threshold differences are 0.05–0.10 eV higher than their primary dissociation counterparts. Specifically, for $n = 8$ the sequential BDE for $Cd^{2+}(H_2O)_6$-H_2O is 0.75 ± 0.03 eV, which is in good agreement with the primary threshold for $n = 7$ at 0.70 ± 0.05 eV. The relative primary–secondary thresholds for $Cd^{2+}(H_2O)_5$-H_2O and $Cd^{2+}(H_2O)_4$-H_2O are 1.00 ± 0.03 and 1.20 ± 0.04 eV, respectively. These are 0.10 ± 0.06 and 0.09 ± 0.06 eV higher in energy than their primary counterparts of 0.90 ± 0.05 and 1.11 ± 0.05 eV for n = 6 and 5, respectively.

The sequential dissociation at $n = 5$ is modeled as a (5,0) → (4,0) + H_2O → (3,0) + $2H_2O$ process; however, the secondary dissociation to form the (3,0) product is complicated by competition with the charge separation process, reaction (3). Unfortunately this sequential competition cannot be modeled using our computational program for data analysis, CRUNCH. Ignoring this complication, we find that the sequential BDE for $Cd^{2+}(H_2O)_3$-H_2O is 1.62 ± 0.03 eV, which is in excellent agreement with the primary dissociation threshold determined without including competition with the charge separation reaction (3), 1.61 ± 0.05 eV for $n = 4$. We anticipate that the competitive shift found for $n = 4$, 0.09 ± 0.03 eV should apply to both of these processes. Additionally, we analyzed the tertiary threshold of the $n = 6$ reactant to provide another sequential BDE for the $n = 4$ complex, Table II. We find the difference between the tertiary and secondary thresholds for $Cd^{2+}(H_2O)_3$-H_2O is 1.78 ± 0.14 eV, 0.16–0.17 ± 0.15 eV higher than the

TABLE III. Comparison of 0 K experimental bond energies (kJ/mol) to theoretical values.

n	Reactant	Product	Exp, primary[a]	Exp, sequential[a]	Exp, weighted average[b]	MP2(full)/SD/6-311+G(2d,2p)[c]	MP2(full)/Def2TZVPP[d]
3	(5,0)	(2,0)		186 ± 14[e]		175.4 (189.6)	185.7 (193.6)
4	(4,0)	(3,0)	146.7 ± 3.9	147.7 ± 4.1[f]	147.2 ± 5.7	144.4 (158.6)	154.5 (162.9)
			146.7 ± 5.6[f]				
5	(5,0)	(4,0)	107.1 ± 4.8	115.8 ± 3.9	112.3 ± 6.1	106.3 (120.9)	110.3 (119.1)
6	(6,0)	(5,0)	86.8 ± 4.8	96.5 ± 2.9	93.9 ± 5.0	97.7 (114.0)	99.1 (108.5)
7	(6,1)_AA	(6,0)	67.5 ± 4.8	72.4 ± 2.9	71.1 ± 5.0	71.1 (80.2)	75.6 (82.7)
8	(6,2)_4D_2AA	(6,1)	63.7 ± 5.8	69.5 ± 2.9	68.3 ± 5.2	73.7 (82.5)	76.4 (83.4)
	(6,2)_2D,DD_2AA	(6,1)	64.6 ± 5.8			72.7 (81.6)	71.6 (78.5)
9	(6,3) _4D,DD_3AA	(6,2)	58.9 ± 4.8	68.5 ± 4.8	63.7 ± 6.8	67.7 (76.4)	71.8 (78.6)
10	(6,4)_4AA	(6,3)	47.3 ± 4.8	62.7 ± 6.8	52.4 ± 7.8	54.9 (63.6)	58.0 (64.8)
	(6,4)_3AA,A	(6,3)	42.5 ± 4.8			52.8 (59.5)	54.1 (60.9)
11	(6,5)_4AA,A	(6,4)	41.5 ± 4.8			49.2 (55.9)	51.2 (56.2)
MADs	Primary		7.9[g]			7.0 (16.7)[h]	9.6 (16.9)[h]
MADs	Sequential					4.8 (8.3)[h]	4.2 (9.3)[h]
MADs	Weighted average					3.5 (12.5)[h]	5.8 (13.0)[h]

[a]Values from Table II.
[b]Weighted average of the primary and sequential BDEs.
[c]MP2(full)/SD/6-311+G(2d,2p)//B3LYP/SD/6-311+G(d,p) level. ZPE corrected. Values listed with (without) cp correction.
[d]MP2(full)/Def2TZVPP//B3LYP/Def2TZVP level. ZPE corrected. Values listed with (without) cp correction.
[e]Tertiary sequential energy including an estimated competitive shift of 19.3 ± 2.9 kJ/mol.
[f]Values including an 8.6 ± 2.9 kJ/mol correction for competition.
[g]Mean absolute deviation between primary and sequential BDEs.
[h]Mean absolute deviation between experiment and theory with (without) cp correction.

primary and sequential thresholds, just outside the experimental uncertainty. This process should also be influenced by competition with charge separation and therefore should also have the 0.09 ± 0.03 eV competitive shift applied.

Because of the contamination discussed above, no secondary threshold was available for sequential analysis of the (4,0) → (3,0) + H_2O → (2,0) + $2H_2O$ dissociation. In an attempt to provide a bond energy for the $n = 3$ complex, the tertiary dissociation of the $n = 5$ reactant was analyzed using the sequential model, Table II. In a previous analysis of higher order dissociations of the $K^+(NH_3)_n$ system, where n = 2–5, the absolute tertiary and quaternary thresholds were high (as is commonly found) and the relative energies were also somewhat high (and increasing with the order of the process), but within experimental uncertainty of values determined from lower order processes.[48] In the sequential dissociation of the $Cd^{2+}(H_2O)_5$ reactant, the tertiary threshold for the formation of $Cd^{2+}(H_2O)_2$ was analyzed, where the relative tertiary–secondary sequential BDE for $Cd^{2+}(H_2O)_2$-H_2O is 2.13 ± 0.14 eV. This sequential dissociation is complicated by reaction (3) and possibly reaction (4) in a similar fashion to the sequential BDE of $Zn^{2+}(H_2O)_5$-H_2O, which was found to have an experimental competitive shift of 0.20 ± 0.03 eV.[49] Using this analogous competitive shift of the Zn^{2+} system, we estimate that the BDE of $n = 3$ is closer to 1.93 ± 0.14 eV. The sizable experimental uncertainty found for this dissociation as well as the tertiary–secondary energy for $Cd^{2+}(H_2O)_3$-H_2O is a result of the scatter in the cross sections resulting from the needed zero pressure extrapolation, which is appreciable for a tertiary water loss process. Both tertiary processes were also modeled using raw data at the lowest Xenon pressure, ~0.05 mTorr, although here the thresholds for both the secondary and tertiary processes were not fit with high fidelity because of the low energy features in the threshold regions resulting from multiple collisions.

L. Comparison of bond dissociation energies: primary versus sequential

The sequential model has been proven to give accurate experimental BDEs for singly charged systems metal systems[48] and was used in our previous study on Zn^{2+} hydration.[26] For Cd^{2+} hydration, the sequential BDEs are 1–15 kJ/mol higher in energy than the corresponding primary values, Table III, with a mean absolute deviation (MAD) of 7.9 kJ/mol for $n = 4$–10, just outside of experimental uncertainty. The largest energy differences between the two values are seen for the $n = 10$ and 9 complexes, 15.4 ± 8.7 and 9.6 ± 7.7 kJ/mol, respectively.

In the zinc system, a large difference between the primary and sequential BDEs was also observed for the $n = 9$ complex, 17.3 ± 8.2 kJ/mol.[26] It was hypothesized that the presence of higher energy isomers in our reactant ion beams could lead to primary dissociation thresholds that are low by the excitation energies of the higher energy complexes. In contrast, the sequential BDE is not influenced by alternate isomers in the reactant beam because the primary and secondary thresholds are lowered by the same amount of energy, such that the relative measurement of the two thresholds is unaffected. Additionally, these alternate isomers are more common for large values of n, where more hydrogen bonding is possible such that there are more complexes with smaller relative energy differences.

For $Cd^{2+}(H_2O)_9$ and $Cd^{2+}(H_2O)_{10}$, the free energy GSs are higher in 0 K enthalpy by 2–4 kJ/mol and may cause the primary dissociation to be lowered by this amount compared to the sequential model threshold. Thus, this hypothesis does

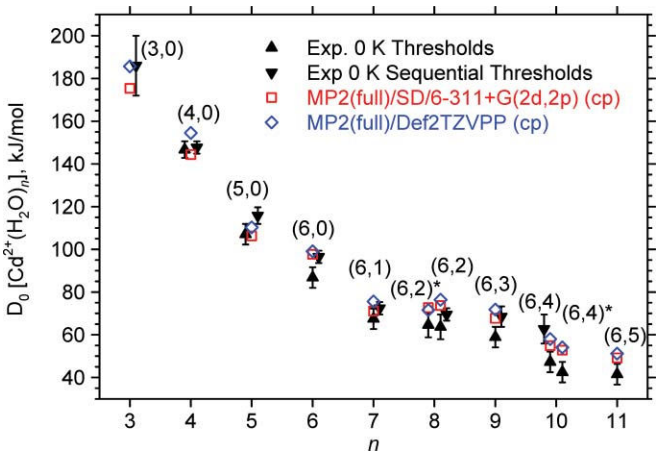

FIG. 6. Comparison of experimental (solid symbols) and MP2(full) theoretical (open symbols) hydration enthalpies at 0 K for both the SD/6-311+G(2d,2p) and Def2TZVPP basis sets. All theoretical results shown are counterpoise corrected. The (6,2)* corresponds to the MP2/Def2TZVPP predicted (6,2)_2D,DD_2AA reactant isomer while (6,2) is the MP2/SD/6-311+G(2d,2p) predicted (6,2)_4A_2AA. The (6,4)* corresponds to the (6,4)_3AA,A reactant isomer which is in thermal equilibrium with the (6,4) = (6,4)_4AA reactant at the MP2(full)/SD/6-311+G(2d,2p) level.

not explain the full magnitude of the difference. Additionally, the sequential BDEs for $n = 5$ and 6 are also 9–10 kJ/mol higher than the primary values and no higher-energy isomers are predicted to be in thermal equilibrium with the reactant GSs at the MP2(full) level. Good agreement between the sequential and primary values is found for $n = 4$, 7, and 8. For $n = 4$, the primary and sequential values are 146.7 ± 5.6 and 147.7 ± 4.1 kJ/mol, respectively, after accounting for the 8.6 ± 2.9 kJ/mol competitive shift noted above. The relative secondary-tertiary BDE for $Cd^{2+}(H_2O)_3$-H_2O is higher at 163 ± 14 kJ/mol, but agrees with the other values within the large experimental uncertainty. The judicious application of the sequential model as an upper limit for higher order processes has been discussed previously.[48]

The sequential BDEs seem to provide accurate upper limits either within or just outside the experimental uncertainty of the primary BDEs, exceeding these by anywhere from 1 to 16 kJ/mol for all values of n examined here. This model seems to be an excellent alternative to obtain thresholds not readily obtained from a primary water loss because of limitations of the ion source, the charge separation process, or signal intensity of the smaller complexes. Additionally, observations and results from this study and our previous study[26] on hydrated Zn^{2+} suggest that this model may in fact be slightly more accurate for complexes where theory predicts multiple high and low-energy isomers to be in thermal equilibrium with each other, as discussed above. It seems low primary BDEs are more common at larger complexes as seen for Cd^{2+} at n = 9–11 and Zn^{2+} for $n = 9$ and 10, where more structures with a variety of hydrogen bonding are in thermal equilibrium. In addition, because of the many low frequency motions of the second shell waters, these larger complexes may be harder to thermalize in our source because of the larger numbers of internal degrees of freedom or may be collisionally excited during extraction from the source much more easily in such a way that their population is no longer in thermal equilibrium before reaching the collision cell. For the above reasons, the sequential BDEs may be more accurate than the primary BDEs at larger complex sizes because the sequential energies should be unaffected by the presence of higher energy complexes.

Ultimately, there is no experimental means of distinguishing the accuracy of the primary versus sequential BDEs for the dissociation of $Cd^{2+}(H_2O)_n$, and hence, we have calculated their weighted average, Table III. The weighted average of these BDEs give MADs between experiment and cp corrected theory of about 5 kJ/mol using either basis set (~12 kJ/mol without cp correction). The weighted average also reflects an increase in the experimental uncertainty for larger complexes where the assumption of a room temperature population distribution may not be accurate, as noted above.

M. Experiment versus theory: water loss

Figure 6 is a direct comparison of experimental and MP2(full) theoretical 0 K hydration energies from Table III. These 0 K bond dissociation energies include ZPE and counterpoise corrections. Single point energies were calculated at the B3LYP, B3P86, and MP2(full) with SD/6-311+G(2d,2p) and Def2TZVPP basis sets from geometry optimizations using B3LYP/SD/6-311+G(d,p) and B3LYP/Def2TZVP levels of theory, respectively. As discussed above, there is evidence that our most accurate interpretation of the data comes from the relative energies and low-energy structures predicted at the MP2(full) level, therefore only the BDEs calculated at the MP2(full) level are given in Table III and Fig. 6. A comparison of the primary BDEs to the MP2(full)/SD/6-311+G(2d,2p) values with and without counterpoise corrections have already been discussed in detail along with a comparison to theoretical values obtained from the literature.[17,25] Clearly there is good agreement between the experimental and theoretical results and the qualitative trends in the experimental values are reproduced in the theoretical BDEs.

The sequential BDE for water loss at $n = 3$ of 186 ± 14 kJ/mol is found by modeling the tertiary dissociation of the $Cd^{2+}(H_2O)_5$ reactant and applying a 19.3 ± 2.9 kJ/mol competitive shift found an analogous dissociation in the zinc hydration study, as explained above. This higher order sequential process is anticipated to be an upper limit to the BDE for this complex size as discussed above and agrees within 1 kJ/mol with the MP2(full)/Def2TZVPP result (within 11 kJ/mol of the MP2(full)/SD/6-311+G(2d,2p) result). The experimental BDE for the water loss at $n = 4$ of 146.7 ± 3.9 kJ/mol includes explicit modeling of competition with charge separation. Our previously reported value at $n = 4$ was slightly higher (~1 kJ/mol) because the competitive shift was estimated using that found for the analogous complex size in our zinc hydration study.

Looking at the overall trends in Fig. 6 there are three distinct patterns in the experimental BDEs that are reproduced by the theoretical numbers. These patterns are most likely a consequence of the three distinct types of waters found in the hydrogen bond networks of the predicted GS structures. Moving from $n = 3$ to 6, each BDE decreases from the

TABLE IV. Comparison of 0 K transition state energies to theory and water loss bond energies (kJ/mol).

n	Reactant	Product	Experiment	B3LYP[a]	B3P86[a]	MP2(full)[a]
3	(3,0)	TS[1 + 1]		83.0	83.9	93.6
		$CdOH^+(H_2O) + H^+(H_2O)$		−88.2	−88.1	−74.0
		(2,0)	186 (14)[b]	185.9	188.4	185.7
4	(4,0)	TS[2 + 1]	126.4 (2.9)[c]	128.8	128.5	139.5
		$CdOH^+(H_2O)_2 + H^+(H_2O)$		−23.7	−24.1	−10.1
		(3,0)	146.7 (3.9)[c]	151.7	154.2	154.5
5	(5,0)	TS[2 + 2]	110.0 (2.9)[c]	81.3	78.9	105.0
		$CdOH^+(H_2O)_2 + H^+(H_2O)_2$		−62.9	−66.1	−37.0
		(4,0)	107.1 (4.8)[d]	104.8	106.9	110.3
6	(6,0)	TS[3 + 2]		90.7	86.9	117.2
		$CdOH^+(H_2O)_3 + H^+(H_2O)_2$		−41.5	−46.9	−14.5
		(5,0)	86.8 (4.8)[d]	92.1	93.6	99.1

[a]Single point energies calculated at the level shown using a Def2TZVPP basis set using geometries optimized at a B3LYP/Def2TZVP level. All values are ZPE corrected.
[b]Value taken from Table III using the sequential dissociation model to analyze a tertiary threshold.
[c]Values taken from Table II using competitive dissociation model.
[d]Values taken from Table II using the primary dissociation channel model.

previous complex, consistent with each water dissociating from the complex being directly coordinated to the metal ion, as predicted by the MP2(full) level of theory. The primary BDEs of the $n = 7$–9 complexes are similar, within 10 kJ/mol of each other (sequential BDEs within 4 kJ/mol), because each of these dissociations involves the loss of a second shell AA water molecule. Lowest in energy are the BDEs found for the $n = 10$ and 11 complexes. If the results for $n = 10$ are interpreted as corresponding to the (6,4)_3AA,A complex [the MP2(full)/SD/6-311+G(2d,2p) 298 K free energy GS], then the experimental BDEs for $n = 10$ and 11 are within 1 kJ/mol of each other. This is consistent with the interpretation that both complexes lose a second shell A water molecule, which binds more weakly than an AA water because it has only a single hydrogen bond to the inner shell. Alternatively, the results for $n = 10$ can be interpreted in terms of the (6,4)_4AA complex, predicted to be in thermal equilibrium using either basis set at the MP2(full) level. Now the experimental and theoretical BDEs for $n = 10$ lie below those of $n = 9$ (by 6–11 kJ/mol experimental, 13–14 kJ/mol theory) and above those of $n = 11$ (by 6 kJ/mol experimental, 3–4 kJ/mol theory), Table III. Here an AA water is lost, explaining why it is more strongly bound than the A water of the $n = 11$ complex, but is bound more weakly than those for $n = 7$–9 because this complex is forced to have two inner shell DD water molecules that each share two second shell water ligands. In the case of $n = 10$, there is not sufficient experimental evidence to definitively conclude which of the two possible complexes is actually being probed in our experiments because experiment and theory are self-consistent for both possibilities. It is certainly possible that the experimental results are a superposition of both configurations.

There is little change in our experimental and MP2(full)/SD/6-311+G(2d,2p) theoretical values from our previously reported results.[17] Our experimental primary BDEs agree best with the SD/6-311+G(2d,2p) basis set with a mean absolute deviation of 6.9 kJ/mol and a MAD between the sequential BDEs and theory of 4.8 kJ/mol. Comparisons between experiment and theoretical results from the Def2TZVPP basis set give MADs of 9.0 and 4.2 kJ/mol for the primary and sequential BDEs, respectively. In general, the MP2(full)/Def2TZVPP level gives theoretical BDEs 1–10 kJ/mol higher in energy than those of the MP2(full)SD/6-311+G(2d,2p) level. A similar trend was seen in a recent report on the inner shell hydration energies of Sr^{2+},[59] where BDEs calculated with the MP2(full)/Def2TZVPP basis set were higher by 1–6 kJ/mol over those calculated at MP2(full)/SD/6-311+(2d,2p) for $n = 1$–5 and lower by 1 kJ/mol at $n = 6$. One difference between these two levels of theory is that the counterpoise correction for the SD/6-311+G(2d,2p) basis set is larger, ranging from 7 to 14 kJ/mol, whereas, the correction using the Def2TZVPP basis set is only 4–10 kJ/mol. The larger correction for the SD/6-311+G(2d,2p) basis set is most likely because the basis set is not size consistent for all atoms (unlike Def2TZVPP), and because the basis set on Cd is smaller than the Def2TZVPP basis set.

N. Charge separation barrier heights

Theoretical results for the charge separation processes are compared with experimental results in Table IV. The predicted energetic barriers for $n = 3$, 5, and 6 are relatively constant at 79–91 kJ/mol at the DFT levels and at 94–117 kJ/mol at MP2(full). Similar barrier heights were also calculated for $Zn^{2+}(H_2O)_n$ charge separation when $n = 5$–7, where the predicted barrier heights ranged from 66 to 75 (83–94) kJ/mol at DFT [MP2(full)] levels.[49] In contrast with these similar barriers, the predicted barrier for $n = 4$ is higher in energy by 38–50 kJ/mol and 22–46 kJ/mol, respectively, compared to the $n = 3$, 5, and 6 TSs, Table IV. Examination of the reverse Coulomb barrier shows a more systematic result in which the barrier decreases as n increases, i.e., 171, 153, 144, and 132 kJ/mol for $n = 3$–6, respectively, at the B3LYP level [168, 150, 142, and 132 kJ/mol at the MP2(full) level], agreeing with trends

discussed for Zn^{2+} hydration.[49] In part, this decrease in the reverse Coulomb barrier as n increases can explained by increasing charge delocalization for larger values of n because of the increasing number of waters on each part of the TS and the charge separation products.

The increase in the predicted forward barrier height for the $n = 4$ complex may be understood in part by the $18e^-$ rule, which is fulfilled at the $Cd^{2+}(H_2O)_4$ complex leading to an enhanced stability of the $n = 4$ complex. Thus, the larger barrier height leads to a lower absolute exothermicity for $n = 4$ compared to the values found for $n = 3$, 5, and 6. The stability of the $n = 4$ complex is also evidenced by the relatively large increase (38–47 kJ/mol) in the predicted water loss BDEs from $n = 5$ to 4. Indeed, this increase exceeds that predicted for $n = 4$ to 3, 31–34 kJ/mol, even though water loss BDEs are expected to increase as n decreases.

The experimental measurement of the charge separation TS energy increases by almost 16 kJ/mol from $n = 5$ to 4, changing from 110.0 ± 2.9 kJ/mol for TS[2 + 2] to 126.4 ± 2.8 kJ/mol for TS[2 + 1], Table IV, agreeing with the predicted trends discussed above. There is good agreement in this TS energy between experiment and theory at $n = 4$, with the MP2(full) value being somewhat high (by 13 kJ/mol). For $n = 5$, MP2(full) calculations predict a barrier height that is in best agreement (within 5 kJ/mol) with the experimental TS[2 + 2] barrier, whereas values predicted by both DFT levels are too low by ~30 kJ/mol.

O. Water loss versus charge separation

The 0 K thresholds and theoretically predicted energies for both the charge separation and water loss dissociation pathways are compared in Table IV. For the $n = 3$ complex, there is no experimental barrier height measured for TS[1 + 1] although theory predicts this barrier ranges from 83 to 94 kJ/mol. Some evidence for this process is observed in the dissociations of the $n = 4$ complex, Fig. 1(a), as discussed above. Here, $Cd^{2+}(H_2O)_4$ can dissociate by reaction (1) followed by reaction (4) to form $CdOH^+(H_2O) + H^+(H_2O) + H_2O$, which is calculated to require 235 (248) kJ/mol at the B3LYP (MP2(full)) levels, i.e., the sum of the energy for loss of the water molecule and the TS[1 + 1] barrier height. This prediction is consistent with the increase observed in the $H^+(H_2O)$ cross section near 2.4 eV, as well as a 30% increase in the total cadmium hydroxide cross section occurring at the same energy. The evidence for this reaction is not definitive, however, because the $CdOH^+(H_2O)$ and $H^+(H_2O)$ products can also be formed via an alternative route, namely reaction (3) [forming $CdOH^+(H_2O)_2$ and $H^+(H_2O)$] followed by reaction (6).

$$CdOH^+(H_2O)_2 + Xe \rightarrow CdOH^+(H_2O) + H_2O + Xe. \quad (6)$$

Reaction (6) is predicted to require 91 (99) kJ/mol. When combined with the barrier for TS[2 + 1] from Table IV, the energy for the reactions (3) + (6) pathway is predicted to cost 220 (239) kJ/mol. Thus, the reactions (3) + (6) pathway, predicted to be 9–15 kJ/mol lower in energy than reactions (1) + (4) pathway, is believed to correspond to the observed onset in the $CdOH^+(H_2O)$ cross section above ~1.8 eV in Fig. 1(a), as mentioned above. The experimental data for both the $H^+(H_2O)$ and $CdOH^+(H_2O)$ cross sections are in qualitative agreement with the predicted relative energies between these two sequential processes. Further evidence of reaction (6) is observed in the $CdOH^+(H_2O)$ product cross sections in Figs. 1(b) and 1(c). In both of these cross sections, there are two features that each start ~1 eV (96 kJ/mol) above the more obvious onsets in the $CdOH^+(H_2O)_2$ cross sections, as discussed above, which is in qualitative agreement with the predicted BDE of reaction (6) (91–99 kJ/mol). Further indirect indications of reaction (4) center on the dissociation behavior of the $Cd^{2+}(H_2O)_3$ complex. The experimental water loss BDE for $n = 3$ is 186 ± 14 kJ/mol, in excellent agreement with the bond energies predicted by all levels calculated using the Def2TZVPP basis set, Table IV. Compared to this energy, the predicted barrier of reaction (4) is much lower in energy by 92–105 kJ/mol. In agreement with our qualitative discussions above, this large energetic preference of reaction (4) probably explains the very low observed magnitude of the $Cd^{2+}(H_2O)_2$ product.

At the $n = 4$ complex, experimental and theoretical results both suggest that reaction (2) is energetically favored over reaction (1) by 20 ± 3 and 15–26 kJ/mol, respectively. For $n = 5$, the relative experimental thresholds for reactions (1) and (5) favor the water loss dissociation pathway by ~3 ± 3 kJ/mol. In contrast, theory suggests that the charge separation reaction is energetically favored over the water loss dissociation by 5–28 kJ/mol, depending on the level. As discussed above, the relative apparent thresholds in Figs. 1(b) and 1(c) for these competing dissociations also suggest that water loss is the energetically favored dissociation pathway. No experimental charge separation products were observed in the primary dissociation of $n = 6$ and it does not seem likely that the charge separation reaction is energetically favored over water loss in agreement with the predicted MP2(full) energies (water loss favored by 18 kJ/mol), but contrary to the DFT results (charge separation favored by 1–7 kJ/mol). In agreement with our conclusions above, the MP2(full) theoretical results appear to provide a better quantitative reproduction of experimental results for charge separation than DFT approaches.

The thermal ESI source used in this study is limited to producing complexes of sizes $n \geq n_{crit}$, as demonstrated previously for hydrated Zn^{2+} and in our in-source fragmentation studies.[26,36] For hydrated Cd^{2+}, we are able to generate the $n = 4$ complex, albeit at low signal intensities, suggesting that $n_{crit} \leq 4$. A large discrepancy between the levels of theory in the predicted barrier heights was found previously for hydrated Zn^{2+},[49] which suggests that theory is not adequately describing the barrier heights for charge separation, although for hydrated Cd^{2+}, MP2(full) gives better agreement to the experimental barrier heights and relative energies between the competing channels. Consequently, we use these experimental observations combined with the experimental relative BDE results to conclude that the critical size for charge separation in the $Cd^{2+}(H_2O)_n$ system is $n_{crit} = 4$, where n_{crit} is defined as the maximum-sized cluster for which charge

TABLE V. Conversion of 0 K thresholds to 298 K enthalpies and free energies for the charge separation transition states for $Cd^{2+}(H_2O)_{4,5}$ and water loss dissociations from $Cd^{2+}(H_2O)_n$, where $n = 3$–11. All values in kJ/mol with uncertainties in parentheses.

Reactant	Product	ΔH_0[a]	$\Delta H_{298} - \Delta H_0$[b]	ΔH_{298}	$T\Delta S_{298}$[b]	ΔG_{298}
(3,0)	(2,0)	186 (14)	1.2 (0.4)	187 (14)	28.2 (1.3)	159 (14)
(4,0)	(3,0)	146.7 (3.9)	1.1 (0.4)	147.8 (3.9)	34.2 (1.3)	113.6 (4.1)
	TS[2 + 1]	126.4 (2.9)	−2.9 (0.3)[c]	123.5 (2.9)	20.5 (1.5)	103.0 (3.3)
			1.8 (0.2)[d]	128.2 (2.9)	4.7 (0.3)	123.5 (2.9)
(5,0)	(4,0)	107.1 (4.8)	2.5 (0.6)	109.6 (4.8)	42.6 (1.4)	67.0 (5.0)
	TS[2 + 2]	110.0 (2.9)	−5.2 (0.4)[c]	104.8 (2.9)	24.3 (1.8)	80.5 (3.4)
			0.1 (0.3)[d]	110.1 (2.9)	8.9 (0.6)	101.2 (3.0)
(6,0)	(5,0)	86.8 (4.8)	1.4 (0.5)	88.2 (4.8)	41.4 (1.4)	46.8 (5.0)
(6,1)_AA	(6,0)	67.5 (4.8)	3.5 (0.4)	71.0 (4.8)	36.2 (1.0)	34.8 (4.9)
(6,2)_4D_2AA	(6,1)	63.7 (5.8)	3.9 (0.4)	67.6 (5.8)	43.1 (1.0)	24.5 (5.9)
(6,3)_4D,DD_3AA	(6,2)	58.9 (4.8)	4.1 (0.4)	63.0 (4.8)	42.5 (1.0)	20.5 (4.9)
(6,4)_4AA	(6,3)	47.3 (4.8)	1.7 (0.3)	49.0 (4.8)	32.3 (1.2)	16.7 (4.9)
(6,5)_4AA,A	(6,4)	41.5 (4.8)	1.2 (0.4)	42.7 (4.8)	31.6 (1.3)	11.1 (5.0)

[a]Experimental values from Table III.
[b]Values calculated from the vibrations and rotations calculated at the B3LYP/SD/6-311+G(d,p) level (for water loss energies) and at the B3LYP/Def2TZVP level (for charge separation barrier heights). Uncertainties found by scaling the frequencies up and down by 10%.
[c]Values calculated with the lowest five vibrations of the TS being treated as rotations.
[d]Values calculated using all vibrations.

separation is energetically favored over the loss of one water ligand.[49]

This value agrees with previous work by Shvartsburg and Siu, although they assign this value as a lower limit because the determination depends on instrumental sensitivity and their definition of critical size does not depend on the energetics of the reaction.[9] Shvartsburg and Siu also suggest that the critical size depends directly on the second ionization energy of the metal, a hypothesis pioneered by the Kebarle group[3,4,6] and charge separation mechanism suggest by the Williams group[8] for a series of different metal ions. In agreement with this, hydration studies in our laboratory find the energy dependent critical size changes as $Sr^{2+} < Ca^{2+} < Cd^{2+} < Zn^{2+}$,[49,59,60] an order that also mirrors their second ionization energies.

P. Conversion to 298 K

Using the calculated frequencies and rotational constants of the transition states, a rigid rotor/harmonic oscillator approximation was applied to convert the 0 K primary water loss threshold energies of the $n = 4$–11 complexes, the sequential BDE of the $n = 3$ complex, and the 0 K charge separation barrier heights of the $n = 4$ and 5 reactants to 298 K values in Table V. The uncertainties in these conversion factors are found by scaling the vibrational frequencies up and down by 10%. The conversions to 298 K energies have been reported previously for the Cd^{2+} system;[17] however, the values changed slightly after the GS structures were fully converged and the values listed here should be considered our most accurate. The changes are within the reported uncertainties, such that the overall trends discussed in our previous report have not changed and are therefore not revisited here.

There are two possible conversion values for the charge separation TSs depending on whether the five low frequency torsions are treated as vibrations or rotors. The 298 K energies for the charge separation TSs at $n = 4$ and 5 are 123.5 and 104.8 kJ/mol, respectively, when the five lowest frequency vibrations are treated as rotors. When these vibrations are treated as low frequency torsions, the 298 K energies rise to 128.2 and 110.1 kJ/mol yielding a difference between the conversion values of ~5 kJ/mol. This difference between the two conversion methods along with trends in the entropies of dissociation, $T\Delta S_{298}$, and the ΔG_{298} values are similar to those reported for the charge separation TSs of hydrated Zn^{2+}.[49] Namely, the $T\Delta S_{298}$ values are larger when the first five vibrations are treated as rotors thereby decreasing the ΔG_{298} values compared to results when all vibrations are used in the TS.

IV. CONCLUSIONS

Complementing our previous article on Cd^{2+} hydration,[17] the present study examines collision-induced dissociation cross sections for $Cd^{2+}(H_2O)_n$, where $n = 4$–11, in more detail with regard to the primary charge separation products for $n = 4$ and 5, $CdOH^+(H_2O)_m + H^+(H_2O)_{n-m-1}$, and the sequential loss of two or three waters from the reactant complex, where $n = 5$–11. Compared to our previous study,[17] computations in the present work ensure that all low and high-energy complexes are fully converged after the frequency calculation. These additional calculations change the relative energies by less than 2 kJ/mol for all complexes investigated and did not affect our experimental thresholds and modeling parameters for water loss channels. However, the structures reported in this paper along with the conversion to 298 K energies are our most accurate.

Ordinarily, our best experimental results are believed to correspond to the measurement of primary dissociation thresholds as they have fewer uncertainties regarding the

distribution of energy available to the dissociating species. However, BDEs obtained from our sequential dissociation model of higher order thresholds provide relatively good agreement with results determined from the primary dissociation channel. The sequential values are slightly higher than the primary thresholds by 1–16 kJ/mol, where these differences are highest for the larger values of n [as also found for $Zn^{2+}(H_2O)_n$, $n \geq 9$] and for the tertiary–secondary relative energies. The higher sequential bond energies at larger complex sizes may indicate that there are distributions of low and high-energy complexes in these reactant beams, which would lower the primary thresholds by those excitation energies. Because such excitations affect both primary and secondary thresholds equally, it is plausible that the sequential model may be more accurate for BDEs of such complexes.

The trends in the relative BDEs for the $Cd^{2+}(H_2O)_n$ systems exhibit three distinct regions in both the experimental and theoretical values. For $n = 3$–6, the BDEs decrease rapidly with increasing n because the waters are directly bound to the metal, whereas for $n = 7$–9, the waters lost are in the second shell and form two hydrogen bonds to the first shell (AA). For $n = 10$ and 11, the simplest interpretation is that the most weakly bound water ligands are in the second shell forming a single hydrogen bond with the inner shell (A), although there is the possibility that for $n = 10$, the water lost is also AA but must share an inner shell donor with another second shell ligand.

The experimental cross sections show that charge separation occurs at $n = 4$ and 5 and possibly at $n = 3$, although definitive observation of the latter is obscured because the same products are also formed by alternative lower-energy routes. The molecular parameters for the tight TSs associated with charge separation are calculated and used to analyze the product cross sections for the CID of $Cd^{2+}(H_2O)_4$ and $Cd^{2+}(H_2O)_5$ by including the competition between water loss and charge separation reactions. Accounting for this competition is necessary for obtaining accurate bond energies of these complexes. On the basis of these experimental thresholds, the $Cd^{2+}(H_2O)_n$ system is determined to have a critical size of $n_{crit} = 4$ for the charge separation reaction. The predicted reverse Coulomb barrier for the charge separation processes at $n = 3$–6 systematically decreases as n increases, whereas theoretical predictions show that the barriers for the charge separation reactions at $n = 3$, 5, and 6 are similar in energy, while the barrier for $n = 4$ is much higher in energy. It appears that the forward barrier height at $n = 4$ is higher because of the increased stability of this reactant complex as a consequence of the 18 e^- rule. This conclusion is further validated by an increase to the experimental barrier heights for charge separation from $n = 5$ to 4 and by the observation that all levels of theory find a difference between the $n = 3$ and 4 hydration energies that is smaller than the difference between the $n = 4$ and 5 hydration energies, Table IV.

ACKNOWLEDGMENTS

This work is supported by the National Science Foundation, Grant Nos. CHE-1049580 and PIRE-0730072. In addition, we thank the Center for High Performance Computing at the University of Utah for the generous allocation of computer time.

[1] W. Salomons, U. Förstner, and P. Mader, *Heavy Metals: Problems and Solutions* (Springer-Verlag, Berlin, 1995).
[2] J. E. Fergusson, *The Heavy Elements: Chemistry, Environmental Impact, and Health Effects*, 1st ed. (Pergamon, Oxford, 1990).
[3] A. T. Blades, P. Jayaweera, M. G. Ikonomou, and P. Kebarle, Int. J. Mass Spectrom. Ion Process. **102**, 251 (1990).
[4] A. T. Blades, J. Palitha, M. G. Ikonomou, and P. Kebarle, J. Chem. Phys. **92**, 5900 (1990).
[5] M. Peschke, A. T. Blades, and P. Kebarle, J. Phys. Chem. A **102**, 9978 (1998).
[6] M. Peschke, A. T. Blades, and P. Kebarle, Int. J. Mass Spectrom. **187**, 685 (1999).
[7] M. Peschke, A. T. Blades, and P. Kebarle, J. Am. Chem. Soc. **122**, 10440 (2000).
[8] M. Beyer, E. R. Williams, and V. E. Bondybey, J. Am. Chem. Soc. **121**, 1565 (1999).
[9] A. A. Shvartsburg and K. W. M. Siu, J. Am. Chem. Soc. **123**, 10071 (2001).
[10] Z. L. Cheng, K. W. M. Siu, R. Guevremont, and S. S. Berman, J. Am. Soc. Mass Spectrom. **3**, 281 (1992).
[11] P. E. Barran, N. R. Walker, and A. J. Stace, J. Chem. Phys. **112**, 6173 (2000).
[12] A. J. Stace, J. Phys. Chem. A **106**, 7993 (2002).
[13] N. F. Dalleska, B. L. Tjelta, and P. B. Armentrout, J. Phys. Chem. **98**, 4191 (1994).
[14] N. F. Dalleska, K. Honma, L. S. Sunderlin, and P. B. Armentrout, J. Am. Chem. Soc. **116**, 3519 (1994).
[15] K. P. Faherty, C. J. Thompson, F. Aguirre, J. Michne, and R. B. Metz, J. Phys. Chem. A **105**, 10054 (2001).
[16] C. J. Thompson, J. Husband, F. Aguirre, and R. B. Metz, J. Phys. Chem. A **104**, 8155 (2000).
[17] T. E. Cooper and P. B. Armentrout, Chem. Phys. Lett. **486**, 1 (2010).
[18] D. T. Richens, *The Chemistry of Aqua Ions* (John Wiley and Sons, Inc, New York, 1997).
[19] P. D'Angelo, G. Chillemi, V. Barone, G. Mancini, N. Sanna, and I. Persson, J. Phys. Chem. B **109**, 9178 (2005).
[20] W. W. Rudolph and C. C. Pye, J. Phys. Chem. B **102**, 3564 (1998).
[21] E. P. F. Lee, P. Soldan, and T. G. Wright, J. Phys. Chem. A **105**, 8510 (2001).
[22] T. S. Hofer, H. T. Tran, C. F. Schwenk, and B. M. Rode, J. Comput. Chem. **25**, 211 (2004).
[23] C. Kritayakornupong, K. Plankensteiner, and B. M. Rode, J. Phys. Chem. A **107**, 10330 (2003).
[24] G. Chillemi, V. Barone, P. D'Angelo, G. Mancini, I. Persson, and N. Sanna, J.Phys. Chem. B **109**, 9186 (2005).
[25] C. C. Pye, M. R. Tomney, and W. W. Rudolph, Can. J. Anal. Sci. Spectrosc. **51**, 140 (2006).
[26] T. E. Cooper, D. R. Carl, and P. B. Armentrout, J. Phys. Chem. A **113**, 13727 (2009).
[27] C. W. Bock, A. K. Katz, and J. P. Glusker, J. Am. Chem. Soc. **117**, 3754 (1994).
[28] A. K. Katz, J. P. Glusker, S. A. Beebe, and C. W. Bock, J. Am. Chem. Soc. **118**, 5752 (1996).
[29] M. Pavlov, P. E. M. Siegbahn, and M. Sandstrom, J. Phys. Chem. A **102**, 219 (1998).
[30] S. Lee, J. Kim, J. K. Park, and K. S. Kim, J. Phys. Chem. **100**, 14329 (1996).
[31] M. Hartmann, T. Clark, and R. van Eldik, J. Mol. Model. **2**, 354 (1996).
[32] M. Hartmann, T. Clark, and R. van Eldik, J. Am. Chem. Soc. **119**, 7843 (1997).
[33] D. Andrae, U. Haeussermann, M. Dolg, H. Stoll, and H. Preuss, Theor. Chem. Acc. **77**, 123 (1990).
[34] T. E. Cooper, J. T. O'Brien, E. R. Williams, and P. B. Armentrout, J. Phys. Chem. A **114**, 12646 (2010).
[35] F. Weigend and R. Ahlrichs, Phys. Chem. Chem. Phys. **7**, 3297 (2005).
[36] D. R. Carl, R. M. Moision, and P. B. Armentrout, J. Am. Soc. Mass Spectrom. **20**, 2312 (2009).
[37] K. M. Ervin and P. B. Armentrout, J. Chem. Phys. **83**, 166 (1985).
[38] D. A. Hales, L. Lian, and P. B. Armentrout, Int. J. Mass Spectrom. Ion Process. **102**, 269 (1990).

[39]R. H. Schultz, K. C. Crellin, and P. B. Armentrout, J. Am. Chem. Soc. **113**, 8590 (1991).
[40]M. T. Rodgers and P. B. Armentrout, J. Chem. Phys. **109**, 1787 (1998).
[41]F. Muntean and P. B. Armentrout, J. Chem. Phys. **115**, 1213 (2001).
[42]R. G. Gilbert and S. C. Smith, *Theory of Unimolecular and Recombination Reactions* (Blackwell Scientific, Oxford, 1990).
[43]K. A. Holbrook, M. J. Pilling, and S. H. Robertson, *Unimolecular Reactions* (Wiley, New York, 1996).
[44]S. K. Loh, D. A. Hales, L. Lian, and P. B. Armentrout, J. Chem. Phys. **90**, 5466 (1989).
[45]F. A. Khan, D. E. Clemmer, R. H. Schultz, and P. B. Armentrout, J. Phys. Chem. **97**, 7979 (1993).
[46]M. T. Rodgers, K. M. Ervin, and P. B. Armentrout, J. Chem. Phys. **106**, 4499 (1997).
[47]P. B. Armentrout and J. Simons, J. Am. Chem. Soc. **114**, 8627 (1992).
[48]P. B. Armentrout, J. Chem. Phys. **126**, 234302 (2007).
[49]T. E. Cooper and P. B. Armentrout, J. Phys. Chem. A **113**, 13742 (2009).
[50]M. J. Frisch, G. W. Trucks, H. B. Schlegel *et al.*, Gaussian, Inc., Pittsburgh, PA, 2005.
[51]A. D. Becke, J. Chem. Phys. **98**, 5648 (1993).
[52]C. Lee, W. Yang, and R. G. Parr, Phys. Rev. B **37**, 785 (1988).
[53]K. L. Schuchardt, B. T. Didier, T. Elsethagen, L. S. Sun, V. Gurumoorthi, J. Chase, J. Li, and T. L. Windus, J. Chem. Inf. Model. **47**, 1045 (2007).
[54]C. W. Bauschlicher, Jr., and H. Partridge, J. Chem. Phys. **103**, 1788 (1995).
[55]J. P. Perdew, Phys. Rev. B **33**, 8822 (1986).
[56]C. Moller and M. S. Plesset, Phys. Rev. **46**, 618 (1934).
[57]S. F. Boys and R. Bernardi, Mol. Phys. **19**, 553 (1970).
[58]F. B. van Duijneveldt, J. G. C. M. van Duijneveldt, and J. H. van Lenthe, Chem. Rev. **94**, 1873 (1994).
[59]D. Carl, B. K. Chatterjee, and P. B. Armentrout, J. Chem. Phys. **132**, 044303 (2010).
[60]D. R. Carl, R. M. Moision, and P. B. Armentrout, Int. J. Mass Spectrom. **265**, 308 (2007).
[61]C. C. Pye, personal communication (13 October 2009).
[62]See supplementary material at http://dx.doi.org/10.1063/1.3553813 for a table of all theoretical results and figures showing geometries of all conformers.
[63]Y. Zhao and D. G. Truhlar, Theor. Chem. Acc. **120**, 215 (2008).
[64]Y. Zhao and D. G. Truhlar, Acc. Chem. Res. **41**, 157 (2008).
[65]R. G. Wilson and G. R. Brewer, *Ion Beams with Applications to Ion Implantation* (Wiley, New York, 1973).